Journal of Materials Chemistry B

ROYAL SOCIETY OF CHEMISTRY

REVIEW

View Article Online
View Journal | View Issue

Cite this: J. Mater. Chem. B, 2022, 10, 7473

Nanomaterial integrated 3D printing for biomedical applications

Liwen Zhang, [a] Helen Forgham,[a] Ao Shen,[ab] Jiafan Wang,[ab] Jiayuan Zhu,[ab] Xumin Huang,[a] Shi-Yang Tang, [c] Chun Xu, [de] Thomas P. Davis[a] and Ruirui Qiao *[a]

Received 29th April 2022,
Accepted 31st July 2022

DOI: 10.1039/d2tb00931e

rsc.li/materials-b

3D printing technology, otherwise known as additive manufacturing, has provided a promising tool for manufacturing customized biomaterials for tissue engineering and regenerative medicine applications. A vast variety of biomaterials including metals, ceramics, polymers, and composites are currently being used as base materials in 3D printing. In recent years, nanomaterials have been incorporated into 3D printing polymers to fabricate innovative, versatile, multifunctional hybrid materials that can be used in many different applications within the biomedical field. This review focuses on recent advances in novel hybrid biomaterials composed of nanomaterials and 3D printing technologies for biomedical applications. Various nanomaterials including metal-based nanomaterials, metal–organic frameworks, upconversion nanoparticles, and lipid-based nanoparticles used for 3D printing are presented, with a summary of the mechanisms, functional properties, advantages, disadvantages, and applications in biomedical 3D printing. To finish, this review offers a perspective and discusses the challenges facing the further development of nanomaterials in biomedical 3D printing.

1. Introduction

Three-dimensional (3D) printing, an additive manufacturing technique, has become a versatile and favorable platform to fabricate products for various medical fields; including general healthcare, pharmaceutics, and items required rapidly in response to a viral pandemic.[1,2] The greatest advantage of 3D printing over traditional manufacturing techniques is the ability to rapidly produce custom-designed and patient-specific scaffolds with high accuracy and complexity.[3] For healthcare, 3D printing technology can be used to develop and fabricate living human cells or tissue for regenerative medicine and tissue engineering. The use of 3D printing also promotes the development of disease models, medical instruments, and drug-containing scaffolds in pharmaceutics. Finally, since the coronavirus disease 2019 (COVID-19) pandemic, 3D printing technology has offered an effective solution in the fabrication of a wide range of structures from testing devices to personal protective equipment.[4] The promise of this technology is huge; however, certain issues have been identified with current 3D-printed biomedical devices, such as poor mechanical properties, limited raw materials in fabricating organs and tissues, and notable transplant-induced infection.[5]

The past several decades have witnessed a rapid increase in the development of nanomaterials for applications in multiple biomedical fields.[6–8] A 'win–win' strategy has been the integration of nanomaterials into 3D printing host materials (*e.g.* polymer or ceramic matrices) and the formation of composite 3D printing biomaterials.[9] For example, there are nanomaterial loaded and/or coated 3D-printed scaffolds for disease prevention and treatment. This integrated approach possesses several merits. For instance, utilizing nanomaterials effectively can potentially overcome some of the poor mechanical properties of current 3D-printed implants. Also, although 3D printing technology can create scaffolds with customized geometric complexities, the lack of mechanical integrity and affinity limits its application in healthcare. By incorporating or coating ceramic, metal, and polymeric nanomaterials into the scaffolds it may be possible to modulate the mechanical properties of the 3D-printed scaffolds, thereby creating a structure that is comparable with both the strength and overall composition of native tissues and organs. Nanomaterials also provide unique properties and advanced functions necessary to influence the biological behavior of current 3D-printed objects. For instance,

[a] Australian Institute for Bioengineering and Nanotechnology, The University of Queensland, Brisbane, QLD 4072, Australia. E-mail: r.qiao@uq.edu.au
[b] School of Chemistry and Molecular Biosciences, The University of Queensland, Brisbane, QLD 4072, Australia
[c] Department of Electronic, Electrical and Systems Engineering, University of Birmingham, Birmingham B15 2TT, UK
[d] School of Dentistry, The University of Queensland, Brisbane, Queensland 4006, Australia
[e] Centre for Orofacial Regeneration, Reconstruction and Rehabilitation (COR3), School of Dentistry, The University of Queensland, Brisbane, QLD 4006, Australia

3D-printed materials coated/loaded with metal and ceramic nanoparticles have been found to promote the proliferation and differentiation of cells.[8] Moreover, the antibacterial properties of silver nanoparticles can be used in 3D-printed scaffolds to prevent the onset of bacterial infection, sometimes occurring as a consequence of transplantation.[10,11] To date, 3D-printed scaffolds containing nanomaterials have shown great promise in the prevention of infection,[12] tissue regeneration,[13] drug delivery,[14] and theragnostic.[15,16] But furthermore, 3D printing technology in combination with nanotechnology offers other advantages such as the customization and personalization of medical products, enhanced productivity, and the democratization of design.[17,18] Undoubtedly, the integration of nanomaterials and 3D printing technology will offer great opportunities for the development of innovative nanocomposites with added functionality and ultimately benefit a wide range of biomedical fields.

In recent years, some review papers have reported nanomaterials, 3D printing technology, and biomedical applications.[19–21] Santos *et al.*, in particular, highlighted the potential for an alliance between nanotechnology and 3D printing for personalized medicine.[20] All of these publications focused on discussing biomedical applications of the fabricated products. However, as far as we know, none of them have discussed in-depth the functions and properties of nanomaterials with respect to biomedical 3D printing. Therefore, this review will provide an introduction and a novel point of view predominantly on the biomedical features of these technologies, whilst also incorporating the associated applications of nanomaterials in 3D printing. Herein, we give a brief introduction describing the integration of 3D printing technology and nanomaterials, and review the main biomedical applications of 3D printing. This is followed by a detailed discussion on the various types of nanomaterials used in biomedical 3D printing technology and their important features; and the integrated approaches of two technologies for printing biomedical nano-scaffolds and biomedical applications of 3D-printed nano-scaffolds. We end by describing the challenges and future perspectives for combining nanomaterials and 3D printing technology for biomedical applications.

Ruirui Qiao

Ruirui Qiao is a Group leader and NHMRC Emerging Leadership Fellow at AIBN, the University of Queensland. She received her BSc (2005) and MSc (2007) in Peking University and was a tenured associate professor (2016–2017) and research assistant professor (2007–2015) at the Institute of Chemistry, Chinese Academy of Sciences (CAS), where she received her PhD in 2014. In 2017, she joined ARC Centre of Bio-Nano Science (CBNS), Monash University, as a project co-leader. Currently, she leads a nanobiotechnology research group at AIBN, focusing on the development of functional nanohybrids toward biomedical and clinical translations.

2. Integration of 3D printing and nanomaterials

3D printing is based on the principle of layer-by-layer manufacturing technology that creates objects directly from a digital model.[21] Since the first 3D printing technology was launched in the early 1980s, 3D printing technology continues to evolve and grow in manufacturing industries such as agriculture, healthcare, automotive, and aerospace industries, as well as in the field of medical research.[22,23] In contrast to conventional manufacturing, 3D printing is considered to be low cost, highly efficient, and results in less waste production. Importantly, the cost-effectiveness of manufacturing means that low volume and small batch production is possible, a particularly advantageous feature to those in the research field. Moreover, because the 3D-printed objects are designed from a computer-aided design (CAD) model, it is easy to create fabricated materials with complicated and customized structures.

Commonly used 3D printing techniques, including Fused Deposition Modeling (FDM), Semi-solid extrusion (SSE), Stereolithography (SLA), Selective Laser Sintering (SLS), and Inkjet-based 3D printing, have successfully been used for the development of various biomedical materials (Fig. 1).[24,25] FDM is an extrusion-based 3D printing technology that utilizes the filament produced by thermally melted polymers to produce the 3D object. Due to cost-effectiveness, excellent resolution, and versatility, FDM has been applied in the fabrication of drug-loaded tablets, controlled release drug delivery systems, and patient-specific implants.[26–28] Another extrusion technique, SSE, has been used to fabricate 3D materials by depositing a gel or paste in successive layers.[29] Unlike FDM, the SSE technique is performed under a low printing temperature, making it more appropriate in thermosensitive biomedicine. Additionally, SSE-based 3D printing exhibits great potential in developing bioelectronics for monitoring physiological parameters. Another benefit of both FDM and SSE is that the ink tank and the printbed are independent, making it easier to evenly encapsulate macromolecules, drugs, and other materials in a single product in the process of printing.[29,30]

SLA as a photopolymerization-related printing technique can transform liquid monomers into solid polymeric objects. Generally, SLA requires light-responsive monomers in the liquid resin, a light source, and a common photoinitiator. The photoinitiator is rapidly activated under light irradiation to initiate polymerization in the liquid resin for generating 3D objects. SLA is advantageous over other methods in terms of the ability to create models with high accuracy, complex structures, and excellent surface quality. SLA-produced objects possess great translational potential in dental implants, bone tissue regeneration, muti-drugs tables, and other personalized medicines.[31,32]

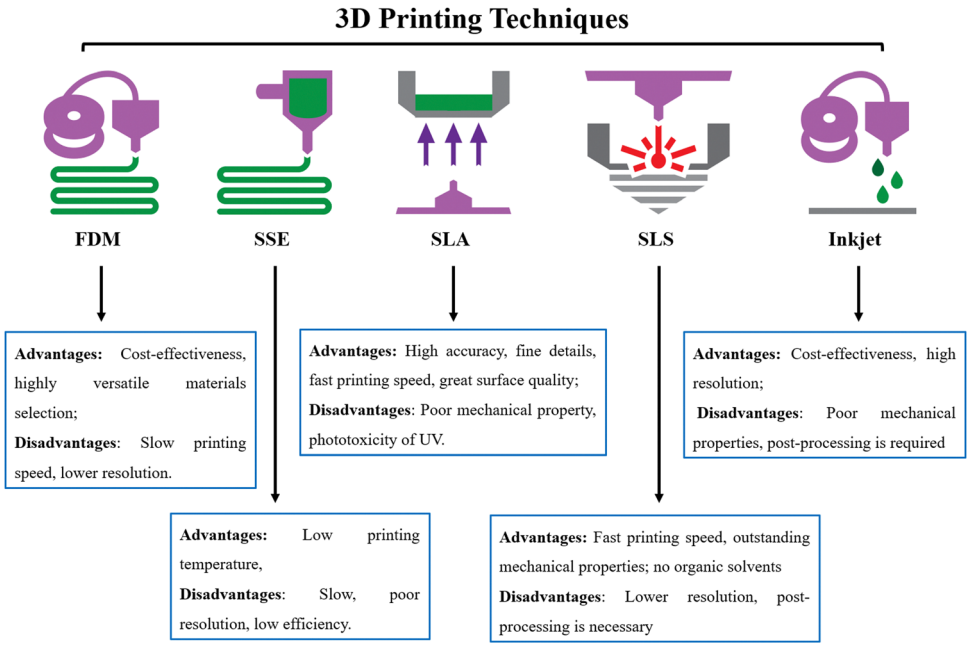

Fig. 1 Summary of advantages and disadvantages of 3D printing techniques.

However, the use of UV sources results in the damage of DNA in biomedical SLA printing. Similar to SLA, the process of SLS uses a laser source to fuse the powder together and build 3D materials.[33] The benefit of this method is that SLS can manufacture objects with fantastic strength and stiffness, particularly the creation of metal-based implants and prostheses with outstanding mechanical properties for a specific patient. On the other hand, the poor accuracy of the laser and powder inevitably limits the details of SLS printed materials.

Inkjet-based 3D printing is a contactless method that utilizes a thermal, electromagnetic, or piezoelectric technique to deposit materials or ink onto the substrate for the fabrication of 3D objects. The low cost, high accuracy, versatility, and biocompatibility of inkjet-based 3D printing allow the production of sophisticated tissues and organs for tissue engineering and regenerative medicine. In addition, other 3D printing techniques, such as digital light processing (DLP),[34] rapid prototyping (RP),[35] and selective laser melting (SLM)[36] have been applied in the manufacturing of biomedical products.

Introducing nanomaterials into 3D printing technology provides a novel strategy for producing high-quality multifunctional integration.[37,38] Nanomaterials are a type of materials with one external dimension measuring between 1 to 100 nm in size.[39,40] They possess ultra-tunable optical emission, high surface area to volume ratio, and other outstanding properties not found in bulk materials.[41] Integrating nanomaterials in the process of 3D printing allows for the fabrication and manipulation of new materials and an enhancement of properties that are desirable for specific applications. Some functional nanomaterials have been employed to obtain or improve the mechanical,[42,43] optical,[44] thermal,[45,46] and electrical properties[47,48] of 3D-printed objects. For instance, considering the brittle nature of photopolymers, it is very difficult to create materials with well-defined mechanical properties *via* SLA printing. The integration of nanomaterials into the liquid resin provides an excellent approach to further improve the mechanical strength of SLA printed materials.[49,50] For example, metal–organic frameworks (MOFs) have been mixed in liquid resin in the process of SLA to fabricate hybrid materials with controllable mechanical properties.[51] While 3D printing offers an effective platform to improve dispersity, stability, and the biocompatibility of nanomaterials,[52,53] manufacturing of nanomaterial-based 3D printing materials remains challenging, as the nanomaterials must first be mixed with the ink/powder before printing and this may result in uneven distribution. In this regard, new methods, such as multiwavelength photopolymerization technology[54] and microfluidics,[55] have been developed to overcome these challenges.

3. Biomedical application of 3D printing

3D printing technology for the fabrication of dental implants and custom prosthetics was first reported in the early 2000s.[56,57] Since then, this technology has revolutionized the medical field and 3D printing now plays a role in a vast number of biomedical applications. In particular, 3D printing is an important part of the production of surgical instruments. Moreover, 3D printing can be used to design anatomical models for trainee surgeons that provide a clearer view of complicated structures, and this offers significant educational value in medical teaching and training.[18] 3D printing is also used in medical imaging and pharmaceutical development, to design custom-fit prosthetics and is under pre-clinical investigation for medical implants such as pacemakers.[58–60]

Importantly, 3D printing has already been approved by the FDA for printing bolus material used in radiotherapy to increase skin exposure[57,61] and 3D-printed dental crowns and implants are now routinely developed by manufacturers to fix or replace the damaged teeth of patients. Additionally, customized hearing aids and orthodontic braces made by 3D printing have also become more commonplace within the healthcare setting.[62–64] The benefits of dental production in particular come down to high efficiency and productivity that permits the modeling of complicated implants within a matter of hours.[65] This ensures that patients do not have to wait long periods for their crowns or implants to be ready. The CAD model is an open-source platform that medical workers and researchers can easily access and download, and this aspect combined with the notable reduction of the production cost associated with 3D printing should mean that in the future things like dental products, small-scale medical devices, and research models will get more affordable for patients, doctors, and researchers alike. One of the most promising future applications for 3D printing is in tissue engineering. Although bioprinting of replacement tissue and organs is still in its early stage, scientists have already printed some superficial tissues and organs. These include knee meniscus, heart valves, spinal disks, other types of cartilage and bone, and an artificial ear.[17,66] 3D-printed materials can also be used to provide an additional barrier between drugs and tissues and be used to control and prolong drug release. For example, Ursan *et al.* demonstrated that Dexamethasone and Levofloxacin-based 3D-printed materials obtained a two-stage release profile and extended drug delivery profile.[67]

In summary, the introduction of 3D printing to the medical field has already resulted in the generation of several important products that have improved patient treatment and well-being. However, there are also some important pre-clinical tools in the pipeline that one day could revolutionize patient care and importantly, directly affect patient survival and treatment outcome.

4. The integration of nanomaterials and 3D printing in biomedicine

Nanomaterials can be relatively easily integrated into 3D printing. The types of nanomaterials found in 3D printing include metal nanoparticles, metal oxide nanoparticles, metal–organic frameworks (MOFs), upconversion nanoparticles (UCNPs), and composite nanoparticles (Fig. 2).

4.1 Metal-based nanomaterials

Based on the classification of 'metal-based nanomaterials',[68] metal nanoparticles (MeNPs, *e.g.*, silver, gold, copper, manganese-based nanoparticles), metal oxides nanoparticles (MONPs, *e.g.*, iron oxide, titanium dioxide, zinc oxide nanoparticles), metal sulfide nanomaterials (MeSNs), liquid metal (LM) materials, metal–organic frameworks (MOFs), and composite nanoparticles (CNPs) have been successfully integrated into 3D printing techniques to fabricate composite materials.

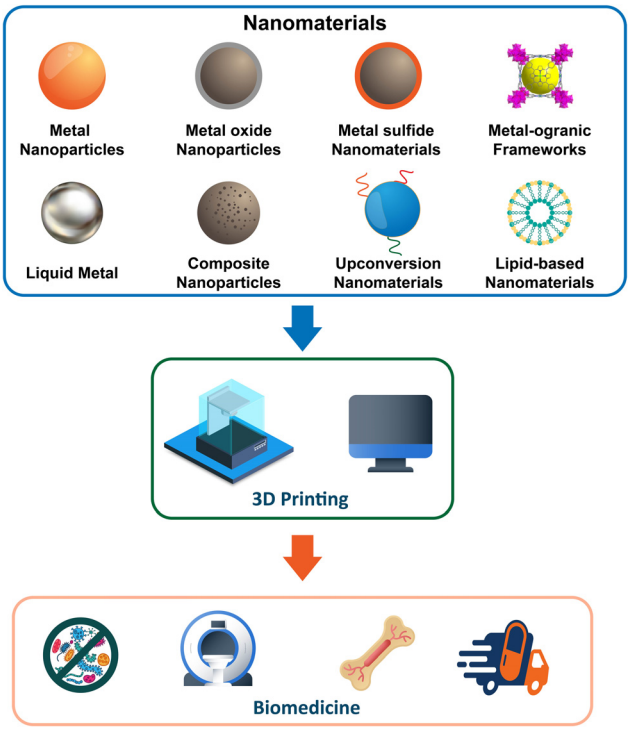

Fig. 2 Current development of integrating numerous nanomaterials with 3D printing technology in biomedicine, including anti-infection, tissue engineering, drug delivery system, medical imaging, and disease treatment.

Moreover, 3D-printed objects designed from these materials have seen a steadily growing rise in interest in a wide range of biomedical fields, including anti-infection, cancer therapy, medical imaging, drug delivery, bone tissue engineering, and biosensors (Table 1).

4.1.1 Metal nanoparticles (MeNPs). In recent years, MeNPs displaying unique mechanical properties have been extensively studied in conjunction with 3D printing techniques. Commonly used MeNPs, such as silver, gold, copper, and manganese-based nanoparticles, have been integrated into SSE, FDM, SLA, and other 3D printing techniques to fabricate multifunctional hybrid materials for an antibacterial effect, tumor therapy, medical imaging, and tissue regeneration. Silver nanoparticles (AgNPs) are well-known for their strong antimicrobial activity against various microorganisms such as bacteria, viruses, and fungi and this effect can be fully exploited by researchers in a range of different fields.[69] For instance, Correia *et al.* produced 3D printed AgNPs scaffolds where 28 nm AgNPs were incorporated into the scaffold using the RP technique. This resulted in printed antimicrobial bone scaffolds designed for bone tissue regeneration.[70] Unfortunately, this strategy of incorporating AgNPs in 3D printed materials is limited by the number of AgNPs released from inside of 3D printed materials. To obtain an effective anti-infection effect, the amount of AgNPs needs to be increased. However, high concentrations of nanoparticles have been shown to cause cellular toxicity and reduce the metabolism of cells. To overcome this issue, Wan *et al.* utilized SSE to fabricate scaffolds with bilayers (Fig. 3(a)).[71] The bottom layer, which was composed of growth

Table 1 Summary of 3D printing technology integrated with some metal-based nanomaterials in biomedical applications

Nanomaterials[a]	Functional properties[b]	Method	3D printing technique[c]	Printed materials[d]	Printed form	Biomedical Applications	Ref.
AgNPs	Antibacterial effect	Incorporation	SSE	GelMA	Scaffold	Anti-infection and diabetic wound healing	71
AgNPs	Anti-infective agents	Coating	FDM	PEEK	Scaffold	Infective bone defect repair	10
CuNPs	Antibacterial effect	Incorporation	SSE	Alginate and bacterial cellulose	Hydrogels	Antimicrobial	74
ZnNPs	Antibacterial effect	Coating	FDM	ABS, Acrylo-nitrile butadiene styrene	Scaffold	Antimicrobial	75
AuNPs	Promoting osteogenic differentiation	Coating	RP	PCL	Scaffold	Bone tissue regenerative therapy	77
AuNPs	CT contrast agent	Incorporation	SSE	GelMA	Scaffold	CT imaging and bone tissue engineering	78
MnNPs	MRI contrast agent	Incorporation	SSE	Alginate-polydopamine	Scaffold	MRI Imaging, photothermal therapy of breast cancer, and tissue repair	16
Fe_3O_4 NPs	Electromagnetic force	Incorporation	SSE	Chitosan	scaffold	Promoting the growth, differentiation, and mineralization of the bone cells	85
SPIONs	Magnetic property	Incorporation	DLP	GelMA	Microswimmer	Theragnostic Cargo Delivery and Release	86,87
USPIOs	MRI contrast agent	Incorporation	SSE	PCL	Scaffold	MRI-guided bile duct repair	89
TiO_2 NPs	Antibacterial effect	Incorporation	SLA	PMMA/PEEK	Dental prosthesis	Dental prosthesis for high antibacterial activity	93
TNTs	Drug carrier	Coating	SLM	Titanium alloy	Titanium implants	Drug release and enhanced bone osteointegration	97
ZnO NPs	Antibacterial property	Incorporation	SSE	Alginate	Scaffold	Wound healing therapy	101
MgO NPs	Cell proliferation	Coating	Melt extrusion	PCL	Scaffold	Improving bone regeneration	102
MoS_2	Photothermal effect	Coating	SSE	AKT	Scaffold	Tumor therapy and bone regeneration	105
LM	conductivity and deformability	Incorporation	SSE	PVA	Scaffold	Multi-modular sensor system	116
ZIF-8	Proliferation and differentiation for osteoblasts	Incorporation	FDM	PCL/DCPD	Scaffolds	Osteogenic differentiation and bone regeneration	123
Fe-MOFs	Drug delivery	Incorporation	DLP	PCL	Scaffold	Antitubercular drug delivery	127
Cu-TCPP	Photothermal effect	Coating	FDM	TCP	Scaffold	Photothermal therapy of bone tumors and bone regeneration	130
Zn-TCPP	Photocatalysts and antibacterial	Incorporation	SLA	PEGDA	Disk	Antibacterial	43
Cu(I)@ZIF-8	The antibacterial effect, cells proliferation, and differentiation	Incorporation	DLP	PLGA	Scaffold	Infected bone repair	135
AgNPs@GO	Antibacterial property and cell proliferation	Coating	SSE	β-tricalcium phosphate	Scaffold	Antibacterial and osteogenic activity	12

[a] AgNPs, sliver nanoparticles; AuNPs, gold nanoparticles; CuNPs, copper nanoparticles; MnNPs, manganese nanoparticles; ZnNPs, zinc nanoparticles; Fe_3O_4 NPs, iron oxide nanoparticles; USPIOs, ultrasmall superparamagnetic iron oxide; SPIONs, superparamagnetic iron oxide nanoparticles; TiO_2 NPs, titanium dioxide nanoparticles; TNTs, titanate nanotubes; ZnO NPs, zinc oxide nanoparticles; MgO NPs, magnesium oxide nanoparticles; ZIF-8, zeolitic imidazolate frameworks-8; GO, graphene; LM, liquid metal. [b] CT, computed tomography; MRI, magnetic resonance imaging. [c] FDM, fused deposition modeling; SSE, semisolid extrusion; RP, rapid prototyping; DLP, digital light processing; SLA, stereolithography SLM, selective laser melting. [d] GelMA, gelatine methacryloyl; PEEK, polyetheretherketone; PCL, poly(e-caprolactone); PMMA, poly(methylmethacrylate); PLGA, poly (lactide-*co*-glycolide); AKT, akermanite; PVA, poly(vinyl alcohol); DCPD, dicalcium phosphate dihydrate; TCP, β-tricalcium phosphate; PEGDA, poly(ethylene glycol) diacrylate.

factor-BB, could promote granulation tissue formation, and improve angiogenesis for diabetic wound healing. Whilst the top layer incorporated AgNPs that could effectively restrain bacterial reproduction for anti-infection. Approximately 91% of growth factor-BB and 19.01 part per billion (ppb) of Ag^+ were sustainably released after incubating the bilayer scaffolds for 14 days in PBS solution. *In vitro*, an antibacterial test demonstrated that the silver-loaded 3D bilayer scaffold restricted *Pseudomonas aeruginosa*, *Staphylococcus aureus*, and *Escherichia coli* infection after 4 h of treatment. The main advantage of the bilayer structure is that it provided a way of reducing the concentration of AgNPs in whole 3D scaffolds whilst maintaining a potent antibacterial effect. In an additional study, Deng *et al.* developed AgNPs coated scaffolds by FDM printing techniques for infection control and

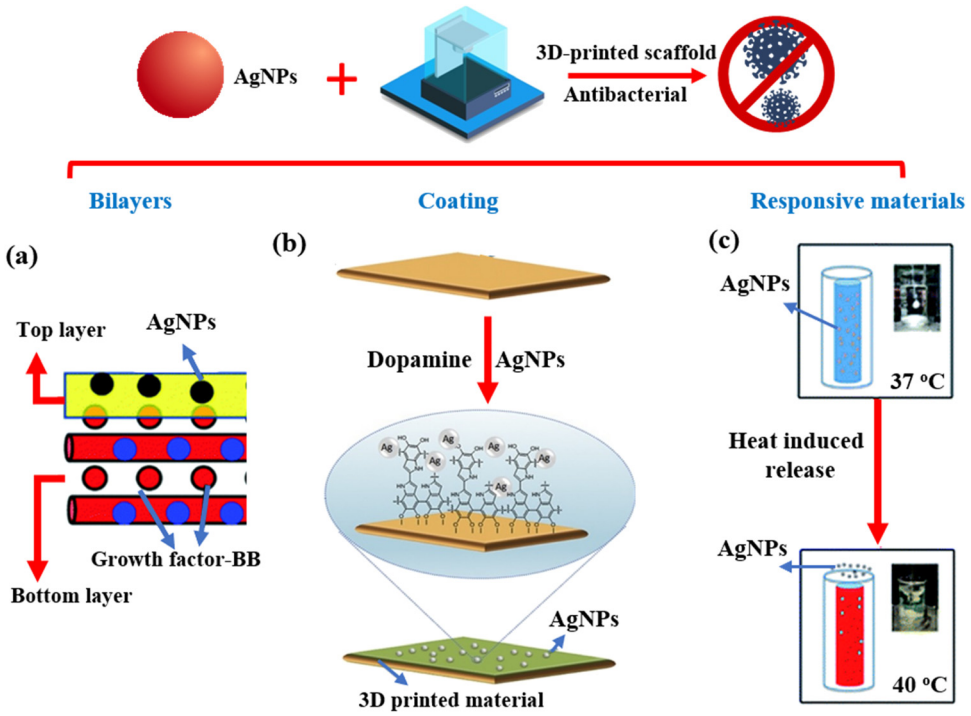

Fig. 3 3D-printed scaffolds containing AgNPs for antibacterial applications. (a) A bilayer scaffold was fabricated for anti-infection.[71] Copyright 2019 Royal Society of Chemistry. (b) AgNPs were coated on the surface of 3D-printed materials for antibacterial activity.[10] Copyright 2017 Elsevier. (c) The thermoresponsive scaffold was printed as a drug delivery system for the AgNPs released under 40 °C.[72] Copyright 2016 Royal Society of Chemistry.

bone repair (Fig. 3(b)).[10] The 3D printed scaffolds were placed in the $AgNO_3$ solution and irradiated with UV light for 30 min to allow for the deposition of AgNPs onto the surface of the scaffolds. AgNPs on the scaffolds were maintained after 15 days of immersion, indicating excellent stability using this approach. AgNPs were homogeneously anchored on the surface of scaffolds by catecholamine chemistry so that they could have direct contact with bacterial cells to achieve antibacterial contact-killing and release-killing effects. The antibacterial tests displayed an obvious inhibition zone (14 mm in diameter) after 24 h incubation of AgNP coated 3D scaffolds with both *E. coli* and *S. aureus*, indicating a significant antibacterial effect on Gram-positive and -negative bacteria. Importantly, AgNPs with a low concentration (1 mM) did not impede MG-63 cell proliferation and osteoblastic differentiation within the scaffolds.

Responsive scaffolds offer another promising design strategy for maximizing the utility of antimicrobial nanomaterials and improving the overall properties of the scaffolds. Utilizing SLA, Ding *et al.* developed scaffolds with inner chambers for thermo-sensitive drug release (Fig. 3(c)). For an antimicrobial effect, AgNPs with an average diameter of 10.2 ± 2.4 nm were loaded into the inner chambers of scaffolds (inner diameter range from 3.3 to 3.6 mm). This was followed by tetradecyl alcohol which was used to seal the entrance.[72] Tetradecyl alcohol as a thermo-sensitive material could auto-release AgNPs from the inner chambers of the scaffolds at 39 °C to kill bacteria. *In vitro* release profiles indicated that more than 95% of drugs could be rapidly released from the inner chambers in 45 mins when the temperature increased to 39 °C. Moreover, this thermal responsive feature meant some bacteria, such as *S. aureus, Pseudomonas aeruginosa, Shigella spp.*, and *Escherichia coli*, could be effectively inhibited at 39 °C (a temperature associated with fever) rather than 37 °C. *In vivo* experiments confirmed that the AgNPs could be released to kill bacteria after mice and rabbits suffered from a fever caused by severe infection. In another study Deng *et al.* employed 3D printing technology to fabricate porous polyetheretherketone scaffolds with a pH-triggered osteopotentiating coating.[73] AgNPs were decorated on the FDM printed scaffolds as the first layer. Apatite minerals were then used as a coating in the outermost layer to obtain the sandwich-structured composites. The apatite not only provided sufficient doses of osteogenic therapeutic ions (Ca^{2+} and PO_4^{3-}) but also prevented the leakage of Ag^+ from scaffolds under normal conditions. However, once an infection had taken hold, the metabolism of bacteria-induced a decrease in pH. When this happened the smart coating immediately released Ag^+ for an antibacterial effect and simultaneously delivered Ca^{2+} and PO_4^{3-} to promote osteogenicity. Although this study outlines a novel strategy to control the release AgNPs from scaffolds, any further application was hampered by the complex design and cumbersome synthesis of the scaffolds.

Similar to AgNPs, copper and zinc-based nanoparticles were also incorporated into 3D printing materials for antibacterial purposes. For instance, Plaza and co-workers incorporated Cu nanoparticles (10 nm) into SSE printed hydrogels to inhibit the growth of *E. coli* and *S. aureus* strains.[74] In the inhibition halo test, scaffolds containing Cu nanoparticles exhibited a clear

inhibition zone (>100 mm^2) in comparison to a non-inhibition (0 mm^2) without Cu nanoparticles. Cockerill *et al.* developed polymeric scaffolds *via* the FDM technique and then cast zinc on the surface to form biodegradable Zn scaffolds.[75] Zn bio-scaffolds displayed 75% pre-osteoblasts viability in cell experiments, indicating Zn possessed low toxicity and high biocompatibility. A 100% antibacterial rate was achieved after culturing zinc scaffolds with *S. aureus* for 24 h, which can be attributed to the excellent bactericidal killing ability of Zn from printed scaffolds. In summary, the outstanding antibacterial properties and controllable biotoxicity of Ag, Cu, and Zn-based nanoparticles make these scaffolds a promising and practical use of 3D printing methods for tissue regeneration and other structural entities where bacterial invasion is problematic. However, some work remains to be done to ensure that the design and synthesis of these structures and scaffolds is a simple and reproducible process.

Gold nanoparticles (AuNPs) are regarded as one of the most favorable nanomaterials for bone tissue engineering due to their capacity in accelerating osteogenic differentiation and promoting bone generation.[76] Therefore, the introduction of AuNPs into 3D printing technology offers an ideal approach to fabricate scaffolds for tissue repair and bone formation. To this end, Sang *et. al.* utilized RP printing technology to fabricate polycaprolactone scaffolds where AuNPs were situated on the surface of the scaffold.[77] As expected, immunofluorescence verified that coating AuNPs on the surface of the scaffold could significantly improve osteogenic differentiation compared with the uncoated scaffold. *In vivo* micro-computed tomography (CT) imaging identified new bone that had formed around the 3D scaffold surfaces after implanting it into a rabbit with a calvaria bone defect for 4 weeks. Additionally, AuNPs as a contrast agent for research use only are available commercially and have been used for X-rays and are becoming increasingly popular for research-led CT imaging due to high X-ray attenuation.[78] For instance, the gelatin methacrylate (GelMA) scaffolds that were embedded by AuNPs (0.16 mM, 60 nm) were regarded as a contrast agent for enhanced μCT imaging in a bone defect.[79] The *in vitro* cell assay the authors performed demonstrated that the scaffolds could promote osteogenic differentiation of mesenchymal stem cells without promoting biotoxicity after culturing scaffolds with cells over 28 days. Importantly, *in vitro* CT imaging could be used to observe the 3D micro-architecture because of the high concentrations of AuNPs (>0.4 mM) encapsulated within and the high X-ray attenuation of AuNPs. Although higher concentrations of AuNPs were favorable for boosting CT signals, it inevitably reduced cellular metabolic activity. Additionally, due to the photothermal properties of AuNRs, bioprinted objects containing gold nanorods (AuNRs) have been used in early-stage breast cancer therapy.[80] In one study, AuNRs (23×85 nm) were loaded on the top layer of a bioprinted structure and a human epithelial breast-cancer cell line, MCF-7, was cultured in the 3D printed complex tissue. The addition of 808 nm laser irradiation significantly increased the temperature of the bio-printed material, resulting in thermal damage-related cell death of the MCF-7 cells.

Additional photothermal responsive metals have also been investigated for various multifunctional applications within the biomedical field. By using the inkjet-printed method, Luo *et al.* reported the development of scaffolds incorporated with manganese-based polydopamine nanoparticles. In this example, the scaffolds were investigated for tumor photothermal therapy in combination with both magnetic resonance (MRI) and photoacoustic dual-modality imaging.[16] As Mn-based nanomaterials are widely used as responsive magnetic resonance imaging (MRI) contrast agents, the scaffolds containing Mn^{2+} demonstrated a strong MRI signal after being implanted within a tumor-bearing mice model. In summary, strategies that utilize nanoparticles with inherent imaging properties to observe printed materials *in vivo*, are a very promising prospect for determining the clinical effect of implanted scaffolds used for treating a range of different ailments.

4.1.2 Metal oxide nanoparticles (MONPs). Alongside pure metal nanoparticles, MONPs have been also reported as an important addition to 3D printing in biomedicine. Specifically, the unique magnetic properties of iron oxide nanoparticles (Fe_3O_4 and γ-Fe_2O_3) are of great interest in disease diagnosis and the design of therapeutics.[81] Magnetic iron oxide nanoparticles once integrated into 3D-printed materials proffer different biomedical functions, including magnetic fluid hyperthermia, stimulating stem cell proliferation, and providing contrast for MRI. To this effect, Yang *et al.* embedded Fe_3O_4 nanoparticles into implantable mats for magnetic hyperthermia.[82] The magnetic mats at a size of 10×10 mm were manufactured using electrohydrodynamic jet printing technology by mixing 6 mmol L^{-1} of Fe_3O_4 nanoparticles with a polycaprolactone solution. Subsequently, the temperature of 3D-printed mats could be raised to 45 °C when placed under an alternating magnetic field (580 kHz, 10 kA m^{-1}) for 45 min. Notably, it has been shown previously that temperatures of between 41–47 °C can cause tumor cell death during hyperthermia therapy.[83] A measurement of cytotoxicity confirmed that magnetic hyperthermia could induce 46% HCT-116 cell death under an alternating magnetic field for 45 min when the cells were cultured together with the mats (6 mmol L^{-1} of Fe_3O_4). *In vivo* studies, a significant remission and reduction in tumor sizes alongside prolonged survival was observed in the mice implanted with 3D-printed mats and treated under alternating magnetic fields. Dong *et al.* also utilized hyperthermia to treat osteosarcoma (Fig. 4(a)).[84] In their study, both calcium peroxide (CaO_2 nanoparticles, $\sim$20–30 nm) and Fe_3O_4 nanoparticles ($\sim$150 nm) were loaded into a mesoporous 3D-printed scaffold. The hyperthermic ability of Fe_3O_4 nanoparticles was used to ablate tumors under a magnetic field, whilst CaO_2 regarded as a hydrogen peroxide source was used to generate highly toxic hydroxyl radicals *via* a Fe_3O_4 nanoparticle-mediated Fenton reaction. This meant that the 3D-printed scaffold could be considered as a dual-purpose treatment to target osteosarcoma; first Fe_3O_4 nanoparticles mediated magnetic hyperthermia and second through the production of hydroxyl radicals in chemodynamic therapy. *In vivo* experiments suggested that tumor growth was inhibited by 91.3% on day 14 when taking advantage of the synergistic effect produced by toxic hydroxyl

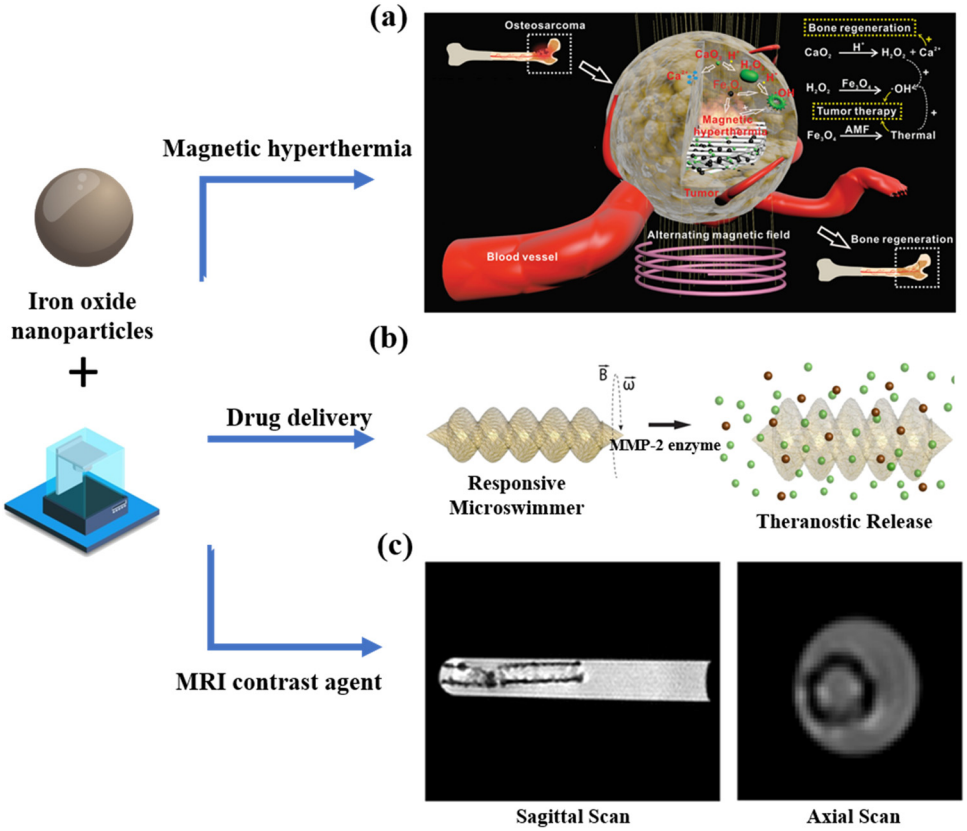

Fig. 4 Biomedical applications of 3D-printed scaffolds containing iron oxide nanoparticles. (a) 3D-printed scaffolds co-loading with CaO_2 and Fe_3O_4 nanoparticles were applied in cancer therapy and bone regeneration.[84] Copyright 2019 Wiley. (b) A microswimmer with SPIONs was printed under rotational magnetic fields for theranostic cargo delivery and release.[86] Copyright 2019 American Chemical Society. (c) *In vitro* MRI of the USPIO-based scaffold.[89] Copyright 2020 IOP Publishing.

radical production and hyperthermia. Alongside magnetothermal therapy, a magnetic stimulus is also a novel approach to promote cell growth and proliferation. For instance, Lin *et al.* created a chitosan-based scaffold that they embedded with Fe_3O_4 nanoparticles (~408 nm) *via* SEE printing technology.[85] When bone cells were cultured on the scaffold (diameter × height = 12 × 2 mm) and exposed to an electromagnetic force (3.0 mA, 30 V, 75 Hz, pulse width = 1.3 ms) for at least 7 days, the DNA assay revealed a higher proliferation and differentiation rate for the bone cells on the scaffolds under an electromagnetic force than those cells without any exposure. Importantly, this study also suggested that electromagnetic force can help bone cells to produce more collagen and mineralization.

Superparamagnetic iron oxide nanoparticles (SPIONs, hydrodynamic diameter range: 10–100 nm) have proven highly promising for inclusion in 3D printing technology and drug release.[86] For example, the two-photon direct laser writing technique has been employed to make magnetic microswimmers for light-triggered drug release.[87] In this work, functionalized SPIONs (~50 nm, 5 mg mL^{-1}) that were embedded into microswimmers (length × outer diameter = 20 × 6 μm) provided the magnetic mobility for controlling the precision and steerability of microswimmers under a 10 mT rotating magnetic field. Subsequently, the anticancer drug, azide-modified doxorubicin (DOX), was anchored on the surface of microswimmers using photocleavable linkers. The DOX could be released from microswimmers once photocleavable linkers were decomposed under light irradiation. The authors demonstrated that DOX release reached about 60% when illuminated with a light (λ_{max} = 365 nm) wavelength for 5 min. Similarly, Ceylan *et al.* fabricated biodegradable micro-robotic microswimmers containing SPIOs for theragnostic cargo delivery (Fig. 4(b)).[86] The difference in this study is the use of the matrix metalloproteinase-2 enzyme instead of light irradiation to initiate drug release. Iron oxide nanoparticles can also potentially be regarded as an MRI contrast agent for disease diagnosis and monitoring.[88] For example, Li *et al.* fabricated a bilayer scaffold containing ultrasmall superparamagnetic iron oxide nanoparticles (USPIOs, hydrodynamic diameter range: 20–50 nm) to monitor bile duct repair using MRI (Fig. 4(c)).[89] The encapsulated USPIOs meant that the 3D-printed scaffold structures could be observed through T_2-weighted MR imaging. Meanwhile, the degradation of scaffolds could be monitored by MR imaging in real-time. Importantly, this method provides a promising and highly relevant approach to evaluating the function and biosafety of 3D-printed materials *in vivo*.

Titanium dioxide (TiO_2) based nanostructures have been applied in dental implants and bone regeneration due to their

good mechanical strength, outstanding antibacterial properties, and enhanced osteoblast adhesion, proliferation, and differentiation.[90–92] In light of these important characteristics, Totu *et al.* used an SLA printer to build a dental prosthesis containing 0.4% TiO_2 nanoparticles with sizes ranging from 56 to 170 nm. The prosthesis demonstrated excellent antibacterial effects, effectively suppressing the propagation of the *Candida Scotti* strain.[93] However, more robust mechanical and biocompatibility experiments still need to be carried out to determine fully the clinical translatability of this work. In an additional study, Chen *et al.* used an SLA 3D printer to manufacture composite resins containing TiO_2 nanoparticles (~30–40 nm) for promoting antibacterial activity.[94] In contrast to pure TiO_2 nanoparticles, the 3D-printed materials displayed more significantly robust antibacterial properties culminating in the extermination of approximately 99% of bacterial pathogens (*S. aureus* and *E. coli*.) under dark conditions within 12 h. This result was attributed to the synergistic antibacterial effect of both the polymer resin and TiO_2 nanoparticles in the printed products. In conclusion, these studies promote the use of TiO_2 nanoparticle-based 3D SLA technology in providing an easy approach to creating dental models and overcoming the problem of infection in implants.

Titanium dioxide nanotubes (TNTs),[95] have also shown great potential for use in 3D printing thanks to their vertically aligned nanotube, hollow internal structures, versatile diameters, and thicknesses.[96] The most obvious difference between TNTs and other metal-based nanoparticles is the unique structure, where the top is open and the bottom is closed. This specialized structure provides an interesting microenvironment for loading and releasing drugs. Maher *et al.* have created implants using titanium alloys based on SLM printing technology.[97] In this process, TNTs with diameters of 10–300 nm and lengths of 0.5–300 μm were positioned on the surface of implants. Next, two types of anticancer drugs, DOX and an apoptosis-inducing ligand (Apo2L/TRAIL) were positioned inside the hollow nanotubes of TNTs. The *in vitro* release profile revealed two-phase behavior with a quick-release phase in the first 6 hours (40% of DOX and 70% of Apo2L/TRAIL) and a slow-release phase over several days. The *in vitro* study also demonstrated that 3D-printed TNT implants containing two anticancer drugs not only improved bone osseointegration but also showed great anticancer efficacy. Inevitably, concerns about this unique structure and the propensity to leak drug from the top side of TNTs needs to be addressed. In this respect, in an alternative study, titanium scaffolds with vertically aligned TNTs were fabricated using SLM 3D printing technology for use in early osseointegration (Fig. 5).[98] Specifically, TNTs were synthesized using the electrochemical anodization method before inclusion with the 3D-printed titanium substrates. Next, a drug, 1α,25-dihydroxyvitamin D3 (VD3) previously shown to improve osteoblast and osteocyte maturation, was encapsulated within the nanochannels of the TNTs. To close off the top of the

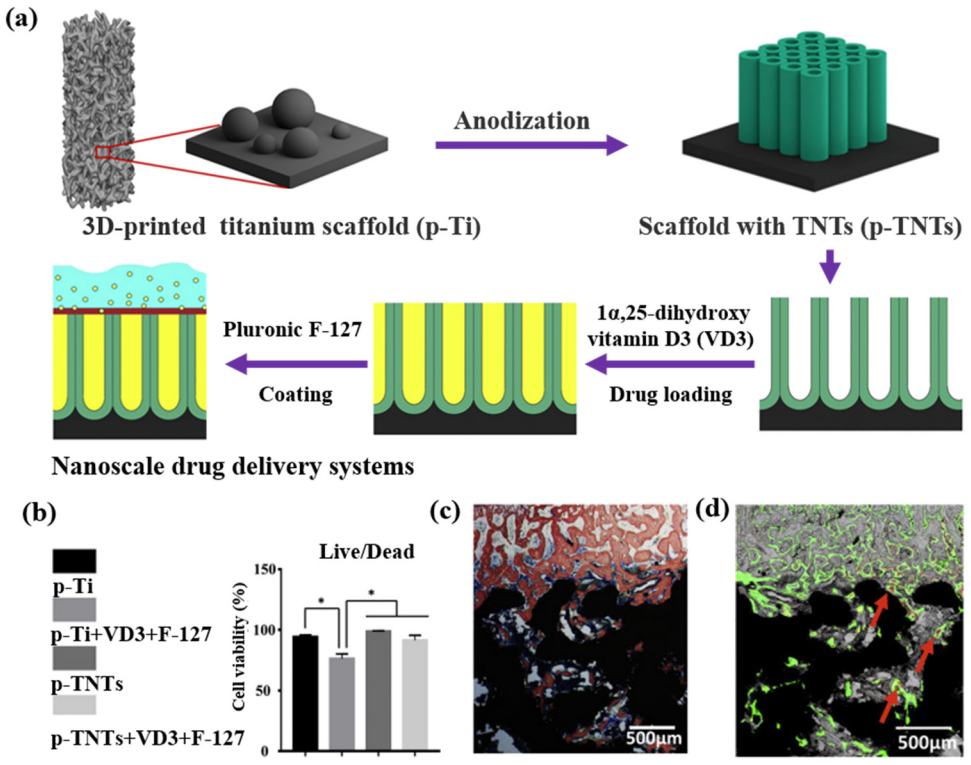

Fig. 5 3D-printed TNT scaffolds for early osseointegration. (a) Schematic illustration of printing titanium scaffolds with vertically aligned TNTs as nanoscale drug delivery systems, selecting VD3 as a model drug and pluronic F-127 as a "bio-cap" to block channels of TNTs. (b) The viability of MC3T3-E1 cells was evaluated by a live/dead assay. (c) Van Gieson staining and (d) fluorescent micrographs were used to access the osteointegration and new bone formation around p-TNTs substrates containing VD 3 and F-127.[98] Copyright 2020 Elsevier.

TNTs, a thermosensitive polymer (Pluronic F-127) was applied to create a protective seal on the top channel. Pluronic F-127 as a thermoreversible hydrogel could effectively control the VD3 release of VD3 from nanochannels present in the TNTs at room temperature. The *in vitro* release profile demonstrated that 45% of VD3 was released within the first 12 hours and that the remaining 55% was slowly released between 1 day and 14 day. *In vitro* and *in vivo* biological studies demonstrated that 3D-printed materials containing VD3 significantly enhanced osteogenesis, thereby improving early osseointegration. Similar results were reported by Qin *et al.* with their SLM printed titanium alloy TNT layered fabrications. However, here subsequent coating with hydroxyapatite (HA) led to an additional enhancement in osseointegration.[99] HA modification was a great approach to further promote osseointegration in contrast to traditional dental implants. However, although the osseointegration ability of 3D-printed materials with both TNT and HA was confirmed measuring protein adsorption, cell adhesion, and gene expression; further *in vivo* investigations are warranted prior to them receiving clinical approval.

Notably, other MONPs that can be incorporated into 3D printing to achieve the desired product characteristic include zinc oxide (ZnO) and magnesium oxide (MgO). ZnO nanoparticles are particularly appealing for inclusion as an antibacterial agent in wound healing as they can produce hydroxyl free radicals that inhibit bacterial reproduction at the wound site.[100] In this respect, Cleetus *et al.*, recently used ZnO nanoparticles with an average size of 5 nm encapsulated within 3D-printed materials for antibacterial and wound healing therapy.[101] Bacterial resistance testing on *Staphylococcus epidermidis* demonstrated that a 3D-printed scaffold with ZnO nanoparticles significantly suppressed the bacterial growth in contrast to scaffolds without ZnO nanoparticles. MgO nanoparticles meanwhile can be engrafted onto the surface of silk fibroin and polycaprolactone-blend scaffolds for promoting bone regeneration.[102] *In vitro* studies have shown that Mg^{2+} could be successfully released from bone-tissue engineered scaffolds to improve adhesion, proliferation, and osteogenic differentiation of pre-osteoblasts. The newly formed bone tissue was observed after transplanting scaffolds into rats with a calvarial defect (5 mm) for 12 weeks. In conclusion, there are many different forms of metal oxide materials that can significantly enhance the performance of 3D scaffolds and structures. Most notably, the inclusion of different metal oxides is shown to inhibit bacterial growth and thus their inclusion is warranted and should be encouraged in 3D models designed for a plethora of different biological applications.

4.1.3 Metal sulfide nanomaterials (MeSNs). MeSNs nanoparticles confer absorption in the near-infrared (NIR) region and demonstrate an excellent photothermal conversion efficiency which promotes the use of MeSNs in photoacoustic imaging and cancer photothermal therapy.[103,104] However, the lack of porous structure and desired mechanical properties limits the biomedical applications of MeSNs. To solve this issue, Wang *et al.* modified molybdenum disulfide (MoS_2) nanosheets on the surface of SSE printed scaffolds (diameter × height = 11 × 3 mm) to generate dark black objects for tumor

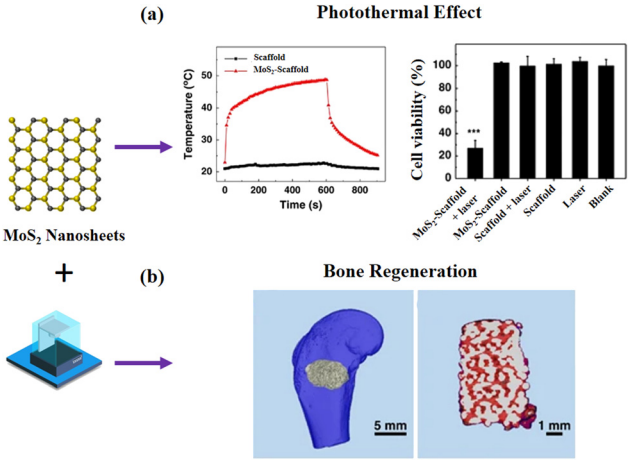

Fig. 6 3D-printed scaffolds containing MoS_2 nanosheets for tumor photothermal therapy and bone regeneration.[105] Copyright 2017 Nature Portfolio.

photothermal treatment and tissue regeneration (Fig. 6).[105] *In vitro* experiments revealed that the temperature of MoS_2 nanosheet-based scaffolds could rapidly increase to above 50 °C under NIR light irradiation (808 nm, 0.6 W cm^{-2}, 10 min), effectively killing 74% of bone tumor cells (Saos-2) and 77% of breast cancer cells (MDA-MA-231). After implanting the scaffold into the central site of the tumor, the temperature of mice could be quickly increased to 50 °C using NIR laser irradiation (0.5 W cm^{-2}, 10 min). Using this technique, tumors were almost ablated after 14 days of treatment. Noticeably, Mo ions were sustainably released from 3D printed materials to further induce proliferation, osteogenic differentiation of bone-forming cells *in vitro* and improve bone regeneration *in vivo*. More recently, Wang *et al.* successfully developed bioactive scaffolds containing MoS_2 nanosheets *via* SSE printing techniques.[106] The scaffolds suppressed osteosarcoma tumor growth when the mice were exposed to 808 nm laser irradiation. Moreover, the scaffold and treatment were beneficial to bone repair in rats with a calvarial defect.

4.1.4 Liquid metal (LM). In contrast to rigid metal nanomaterials, LM materials made from Gallium (Ga) and its alloys such as EGaIn (a eutectic alloy of Ga and Indium) or Galinstan (a eutectic alloy of Ga, Indium, and Tin) are soft due to their fluidic property. Ga liquid metal has attracted widespread interest thanks to its unique characteristics, including low melting point, significant supercooling effect (nanoparticles can remain to be liquid even below −30 °C), high electrical conductivity, great thermal conductivity, and large surface tension.[107–109] Ga liquid metal alloys demonstrate non-toxicity and excellent biocompatibility making them suitable for research in drug delivery, tumor therapy, anti-infection, and other biomedical applications.[110–113] Notably, excellent electrical conductivity enables LM to be successfully used in the fabrication of biosensors.[114] For instance, Jin *et al.* utilized gallium–indium eutectic LM when printing medical devices for nerve electrical stimulations.[115] The 3D medical electronics were directly fabricated *via* injecting the LM-based materials

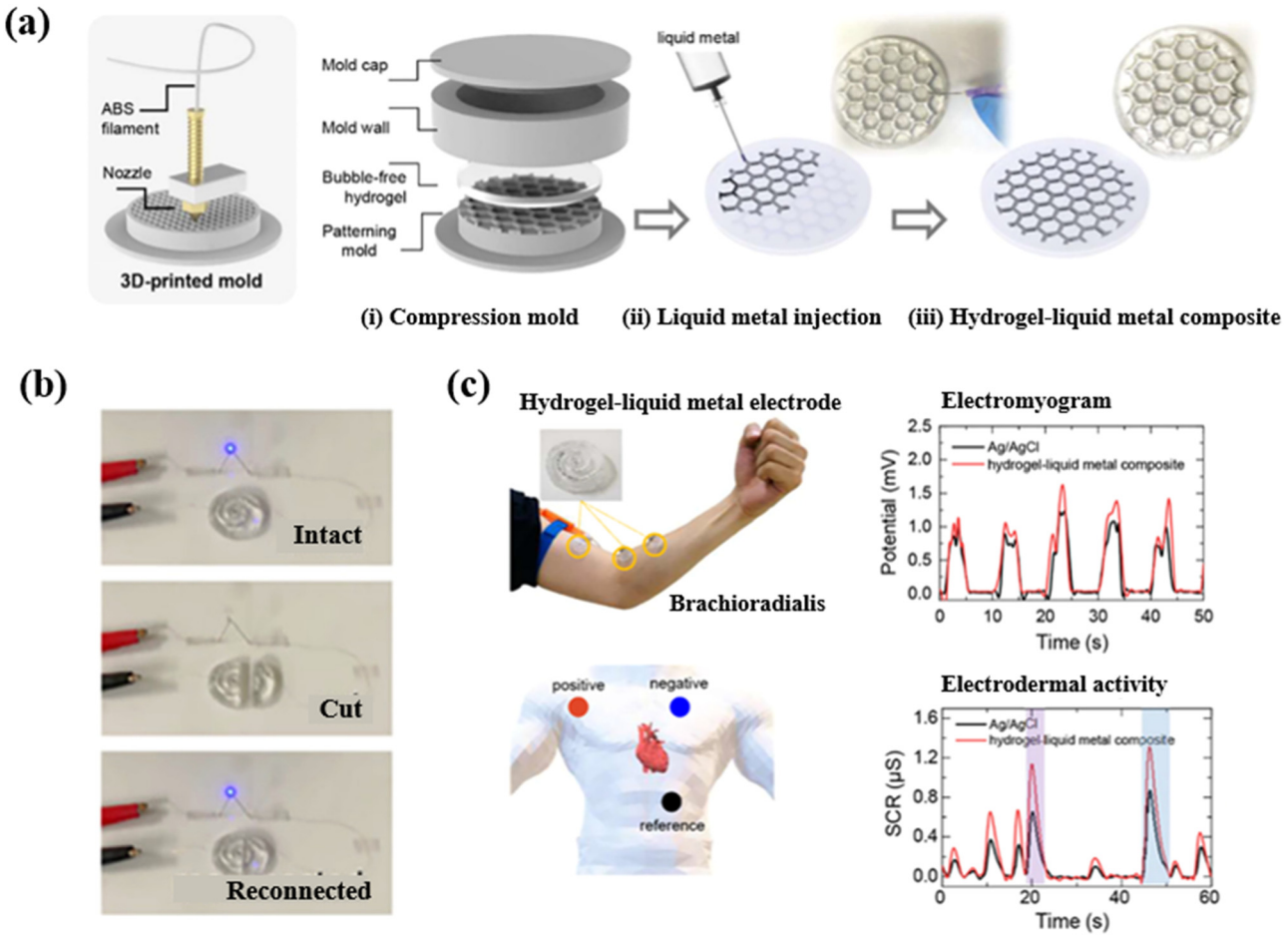

Fig. 7 The hydrogel–LM composite was applied in a multinodular sensor system.[116] (a) Schematic illustration of manufacturing the hydrogel–LM composite by 3D printing technology. (b) The self-healing capacity of the hydrogel–LM composite was evaluated using an LED. (c) Hydrogel–LM composite-based electrodes were used to detect bio-signals. Copyright 2020 American Chemical Society.

into the frog's tissues to electrically stimulate the sciatic nerve, demonstrating the possibility of direct printing LM or its composites for biosensing applications. Taking this approach, Choi *et al.* developed a hydrogel–LM composite using a 3D-printed mold to be used as a self-healable biosensor electrode (Fig. 7).[116] The hydrogel-based mold was created by 3D printing technology, followed by injecting LM into the space of 3D-printed materials to generate the hydrogel–LM composite. Due to the self-healing feature of hydrogels, 3D-printed materials were employed as self-healable electrodes for the customizable sensor system. More importantly, apart from direct printing LM in a hydrogel matrix, 3D printing uncured elastomer filled with micro to nano-sized LM particles was also demonstrated, offering the opportunity to directly create conductive networks with more complex structures and better elastic performance.[117,118] Conductive networks created by mechanically "sintered" LM particles have the potential to allow the composite to act as an electrode to detect various bio-signals, such as electromyogram, electrocardiogram, and electrodermal activity. Given the promise of 3D-printed composites with LM fillers, we believe they will become an important asset in various bioapplications. However, to date this area of research remains largely underexplored.

4.1.5 Metal–organic frameworks (MOFs). MOFs are a novel class of networked hybrid nanomaterials constructed from metal ions/clusters and functional organic linkers.[119,120] High porosity, excellent stability, tunability, and advanced bio-related features make MOFs attractive in bioimaging, drug delivery, biocatalysis, biosensing, and antibacterial applications.[121,122] Thus, 3D printing MOFs are a useful addition to the development of 3D-printed materials for biological applications. For example, Zhong *et al.* used the FDM printing technique to successfully integrate zeolitic imidazolate framework-8 (ZIF-8, ~300 nm), a subclass of MOFs, into composite scaffolds made from polycaprolactone and dicalcium phosphate dihydrate.[123] ZIF-8 based scaffolds could significantly enhance the expression of osteogenesis-related genes and promote the osteogenesis of bone mesenchymal stem cells compared with printed materials without ZIF-8. This is because Zn ions from ZIF-8 have been demonstrated to promote osteogenic proliferation and differentiation of bone cells.[124–126] Fabricated scaffolds containing ZIF-8 could also repair bone tissue in

rabbits with a calvarial defect. Additionally, Peng *et al.* encapsulated Fe-based MOFs into mesoporous bioactive glass scaffolds using DLP printing.[127] This study demonstrated that the composite scaffolds could improve the compressive strength by 3–7 MPa. Antitubercular drug (isoniazid) loaded MOF scaffolds showed a rapid release (>28% isoniazid) on the first day after incubation at 37 °C. These results, alongside their excellent potential for degradability under an acidic pH microenvironment suggest that MOF scaffolds hold great potential for use in the controlled delivery of antitubercular drugs.

Another new subclass of nonporous materials that is being explored in 3D-printed biomedical applications is 2D MOFs nanosheets. 2D MOFs proffer several benefits over conventional 3D analogs, including unique morphological structures, mechanical flexibility, optical transparency, greater surface area, and more active sites.[128,129] Very recently, Dang *et al.* fabricated FDM-based β-tricalcium phosphate scaffolds containing Cu-TCPP (5,10,15,20-(tetra-4-carboxyphenyl) porphyrin, TCPP) for bone tissue regeneration and tumor therapy (Fig. 8(a)).[130] When Cu-TCPP nanosheets were prepared on the surface of scaffolds using a solvothermal method, the Cu ions released from 3D-printed materials promoted bone generation through stimulating osteogenesis and angiogenesis. After transplanting 3D-printed materials (diameter × height = 5 × 8 mm) into the bone defects of rabbits for 8 weeks, new bone-related tissues inside scaffolds were discovered using micro-CT imaging. This result suggested that Cu-TCPP nanosheets from 3D printed scaffolds were beneficial in the generation of new bone. In addition, the photothermal feature of Cu-TCPP nanosheets made the 3D-printed scaffolds kill bone tumor cells under near-infrared (NIR) light irradiation. The result showed that the temperature of scaffolds containing Cu-TCPP nanosheets was rapidly increased to more than 80 °C while illuminated with NIR light (0.9 W cm^{-2}) for 10 min. *In vivo* studies revealed that the temperature in the bone tumor sites with Cu-TCPP nanosheet-based scaffolds (length × width × height = 5 × 2 × 1 mm) significantly increased to 55 °C under NIR light irradiation (0.9 W cm^{-2}, 10 min), effectively ablating tumors and suppressing the regeneration of bone tumor cells.

Apart from functional metal ions, organic ligands of MOFs have been employed in 3D-printed mediated biomedicine. For instance, Zhang *et al.* reported on the synthesis of bifunctional 2D MOFs (Zn-TCPP nanosheets) produced using SLA printing for antibacterial photodynamic therapy (Fig. 8(b)).[43] Due to the excellent photocatalytic activity of metalloporphyrin-based ligands,[51,131,132] Zn-TCPP nanosheets with an average diameter of 600 to 1000 nm and a thickness of 2.7 ± 0.4 nm were used as heterogeneous photocatalysts to mediated photo-induced electron/energy transfer-reversible addition-fragmentation chain transfer polymerization. High monomer conversion (≥80%), low dispersity (<1.10), and excellent end-group fidelity (80%) were achieved in the polymerization process. Additionally, polymeric objects with high resolution and accuracy were manufactured by the Zn-TCPP nanosheet (0.2 mg mL^{-1}) mediated SLA printing technique. The great mechanical flexibility of 2D MOFs meant that the Zn-TCPP nanosheets could be used to improve the flexural and tensile strength of the printed objects. As organic ligands of Zn-TCPP nanosheets could rapidly transform oxygen into singlet oxygen under green light (λ_{max} = 565 nm, 10 mW cm^{-2}), a 3D-printed disk

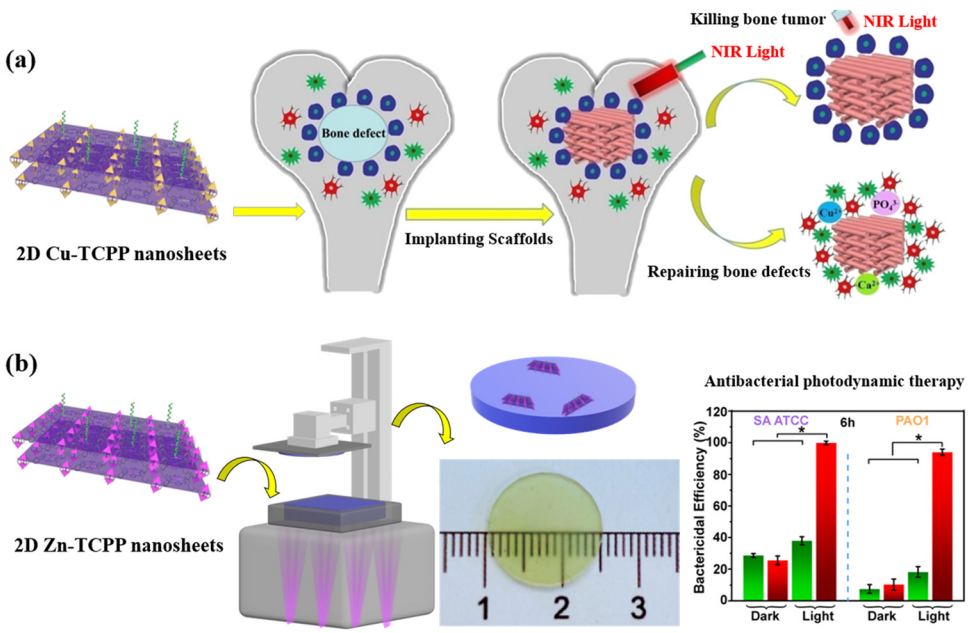

Fig. 8 2D MOF-mediated 3D printing and biomedicine: (a) Illustration diagrams of ablating bone tumors and repairing bone defects by 3D-printed scaffolds containing Cu-TCPP nanosheets;[130] Copyright 2020 IOP Publishing. (b) Zn-TCPP nanosheets acted as heterogeneous photocatalysts to mediate 3D printing and antibacterial photodynamic therapy.[43] The bar graph in green denotes the disk without Zn-TCPP nanosheets, whereas the red color denotes the disk with Zn-TCPP nanosheets. Copyright 2021 Wiley.

(diameter × height = 15 × 0.5 mm) with 0.2 mg mL^{-1} of Zn-TCPP nanosheets could also generate singlet oxygen under the same green light irradiation to effectively suppress bacterial growth using antibacterial photodynamic therapy. Colony-forming unit assays demonstrated that approximately 98% of Gram-positive (*Staphylococcus aureus*) and 94% of Gram-negative (*Pseudomonas aeruginosa*) bacteria on the 3D-printed disk were killed during exposure under green light for 6 h. The authors further compared 2D and 3D Zn-TCPP MOFs in SLA printing. 2D MOFs possess a higher photocatalytic activity and polymerization efficiency than conventional 3D MOFs owing to their greater surface area, better light penetration, and more catalytic sites. In contrast to 3D analogs, 2D nanosheets as heterogeneous photocatalysts could significantly increase the printing speed from 0.05 to 0.24 mm h^{-1}. On the other hand, 3D MOF-printed materials displayed higher flexural and tensile strength in comparison to the printed object catalyzed by 2D MOFs. This is because 3D nanoparticles are able to reduce the size of voids and improve the mechanical strength of printed materials.[133] Taken together, these works provide new horizons in the biomedical field and inspiration to explore further the benefits of multifunctional MOFs in relation to 3D printing.

4.1.6 Composite nanoparticles (CNPs). CNPs, composed of two or more components, have obtained much interest from scientists owing to their advanced features and multifunctional properties when compared to single metal nanoparticles. These features enable CNPs to possess combined or significantly different electrical, chemical, physical, and mechanical properties from single component materials.[134] Recently, researchers have been exploiting the advanced properties of CNPs and combining them with 3D printing techniques. For example, DLP printing was used to create Cu(I)@ZIF-8 scaffolds (diameter × height = 10 × 0.9 mm) used to prevent the onset of bone infection (Fig. 9).[135] The Cu(I)@ZIF-8 nanocomposite with an average size of 85 nm was synthesized by loading cooper inside nanochannels of zeolitic imidazolate framework-8 (ZIF-8), where copper provided an excellent antibacterial effect that suppressed the growth of bacteria.[136] On the other hand, Zn in ZIF-8 presented an osteoconductive effect that was used to promote cell proliferation and differentiation.[137] Therefore, the 3D-printed scaffolds provided a dual function by preventing infection and encouraging bone repair. As with the individual nanomaterials that make up the nanocomposites, nanocomposites could also be coated on the surface of SSE-printed scaffolds to provide various biomedical functions. For instance, homogeneous nanocomposites that were prepared by decorating AgNPs onto graphene oxide (GO) were coated on the surface of bioceramic scaffolds in the Zhang *et al.* study.[12] Benefiting from the antibacterial property of AgNPs and cell proliferation ability of GO, Ag/GO nanocomposites on the surface of scaffolds not only effectively killed *E. coli* cells but also promoted the osteogenic differentiation of rabbit bone marrow stromal cells.

To summarize, 3D-printed products using metal-based nanocomposites have shown great potential in potentiating the effects of current 3D-printed scaffolds. However, the use of nanocomposites in 3D printing remains problematic and

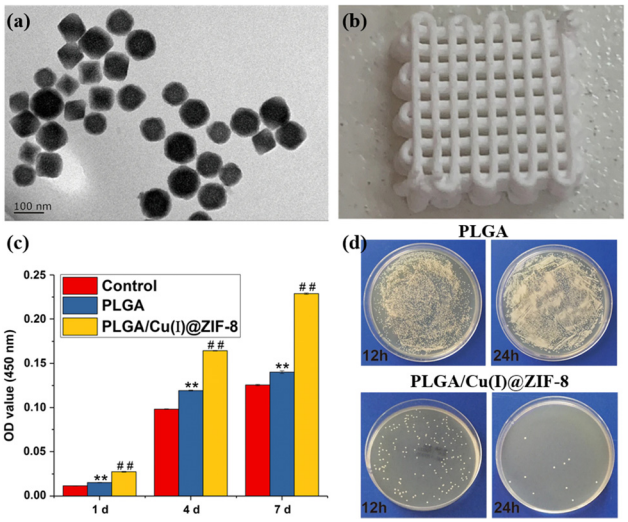

Fig. 9 Cu(I)@ZIF-8 nanocomposite-based scaffolds for infected bone repair.[135] (a) The transmission electron microscope micrograph of Cu(I)@ZIF-8 nanocomposites. (b) The image of a 3D-printed PLGA scaffold with the Cu(I)@ZIF-8 nanocomposite. (c) The cell proliferation of murine mesenchymal stem cells on the PLGA and PLGA/Cu(I)@ZIF-8 scaffolds. (d) The bacterial growth on the surface of PLGA and PLGA/Cu(I)@ZIF-8 scaffolds was measured *via* colony-forming assay after incubating for 12 and 24 h. Copyright 2020 BioMed Central Ltd.

challenges including high viscosity, stability of nanocomposites in the process of printing, and homogeneity of mixed solutions need to be overcome prior to effective translation. In this respect, future research on nanocomposites for 3D printing should consider more closely biostability, toxicity, and overall mechanical strength.

4.2 Upconversion nanoparticles (UCNPs)

UCNPs act as luminescent nanomaterials capable of photon upconversion from low-energy NIR light to high-energy ultraviolet (UV) or visible light.[138,139] Photon upconversion is the most important feature of UCNPs and is highly significant to the biomedical field. UCNPs under NIR excitation has the capacity to emit visible light which can act as an initiator for different photosensitizers. Nigoghossian *et al.* developed UCNP-based scaffolds for photodynamic therapy (PDT) under 980 nm excitation.[140] Here, UCNPs were used as a transducer to initiate a photosensitizer (erythrosine B) in polymerization. When 12.5 wt% UCNPs and erythrosine B are embedded into polymeric materials using FDM technology, a proof-of-concept study confirmed that fabricated scaffolds could generate cytotoxic singlet oxygen under NIR excitation, inducing cell apoptosis. The advantage is that NIR light-mediated PDT holds deeper penetration to the lesion area and lower photo-damage to normal tissue compared with UV/visible light-mediated PDT.[141] This is because the NIR light possesses weaker light scattering, deeper penetration, lower light absorption, and lower background noises in contrast to UV or visible light.[142] Although UV is usually regarded as the light source in SLA and DLP technology, the toxicity associated with UV radiation inevitably impedes their biomedical application. NIR light,

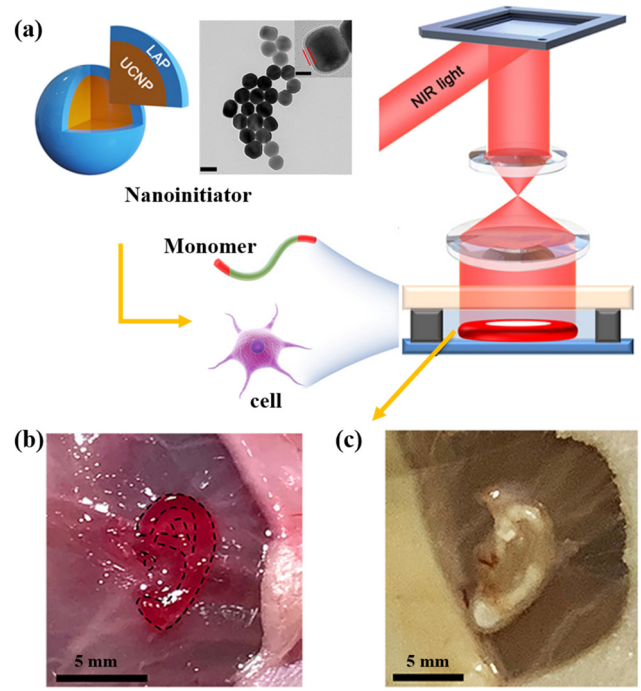

Fig. 10 UCNPs initiated noninvasive 3D bioprinting.[143] (a) Schematic diagram of noninvasive *in vivo* 3D bioprinting that is based on a nanoinitiator mediated photopolymerization under NIR light irradiation. The ear-shaped construct *in vivo* was printed in BALB/c nude mice. (b) The ear-shaped materials were printed in BALB/c nude mice by noninvasive 3D bioprinting. (c) Image of the ear-shaped construct at 1 month. Copyright 2020 Science.

which has deeper penetration and lower damage, is fast becoming a better candidate as an excitation light source to initiate photo-based 3D printing. To this end, Chen *et al.* have developed noninvasive *in vivo* tissue bioprinting based on nanoinitiator mediated photopolymerization under NIR light irradiation (Fig. 10).[143] Firstly, in this study the UV/blue light-sensitive photoinitiator (lithium phenyl-2,4,6-trimethyl-benzoyl phosphonate) was coated on the surface of UCNPs ($NaYF_4$:Yb, Tm, 30/0.3 mole percent) to generate a nanoinitiator with an average particle size of 60 nm. The UCNPs in the core of the nanoinitiator were subsequently shown to upconvert NIR light (λ_{max} = 980 nm) into UV (λ_{max} = 345 and 361 nm), which could then activate the outer photoinitiator to mediate photopolymerization. Next, the nanoinitiator was mixed into the bio-ink to fabricate a customized tissue construct using *in vivo* a digital NIR light photopolymerization (DNP) mediated 3D printing technique. Notably, this approach proved to be noninvasive to manufacture tissues *in situ* without causing any toxicity or damage. The resulting ear-shaped tissue was successfully grafted onto the BALB/c nude mice using DNP-mediated bioprinting where it maintained good morphology. This study epitomizes the future role that this kind of technology can play in the treatment of pinna defects or microtia and opens the door for other opportunities in medical 3D printing of minimally invasive or non-invasive 3D models in medicine.

4.3 Lipid-based nanoparticles (LBNPs)

Good scale-up feasibility, great stability, low toxicity, long drug circulation time, biocompatibility, and biodegradability make LBNPs one of the most promising carriers for drug delivery and

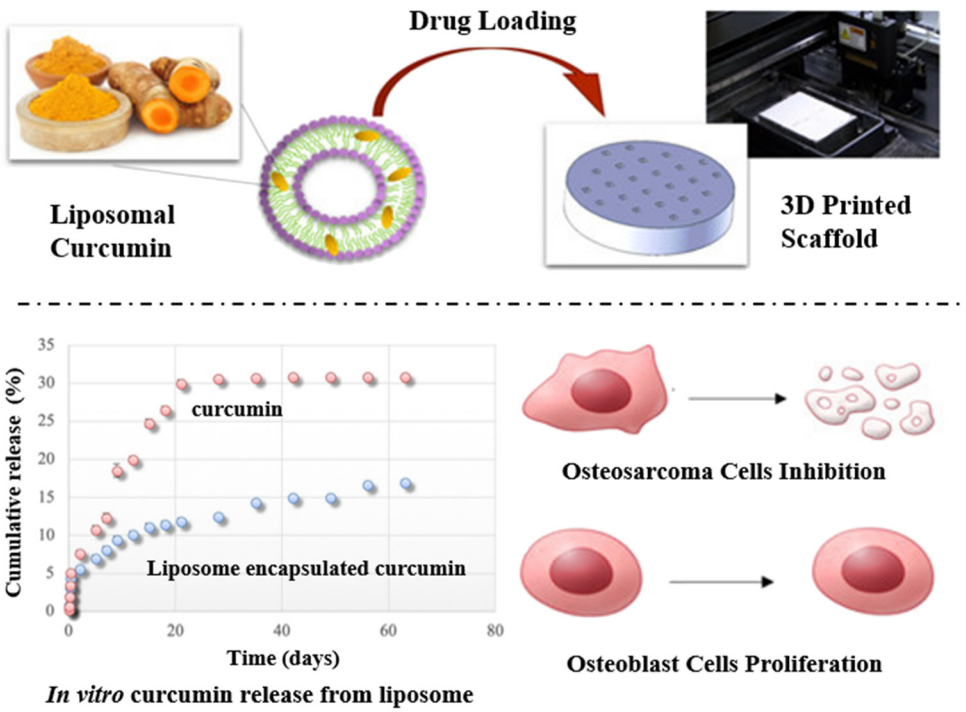

Fig. 11 Schematic illustration of 3D-printed calcium phosphate scaffolds with curcumin-loaded liposome for controlling drug release, suppressing osteosarcoma cells growth, and promoting the proliferation of human osteoblast cells.[146] Copyright 2019 American Chemical Society.

tumor therapy.[144] Liposomes are the most common LBNPs used for the fabrication of 3D-printed scaffolds and as such, there is a raft of literature on their use. One of the best examples of their use comes from Liu *et al.* who designed 3D bio-printed hydrogel patches with various morphologies that were capable of encapsulating anticancer drug DOX-loaded liposomes.[145] Analysis of the drug release profile demonstrated that the DOX was effectively released from 3D-printed patches and interestingly, that the drug release ratio was dependent on the distinct hydrogel morphology. Unfortunately, this result was not further validated by a robust panel of *in vitro* and *in vivo* studies. Recently, Sarkar and Bose successfully encapsulated the anti-cancer agent curcumin inside of liposomes to produce nanocomposites with sizes in the range 40 to 50 nm. Subsequently, the liposomes were homogeneously coated on the surface of 3D-printed calcium phosphate scaffolds (Fig. 11).[146] The 3D printed object could support the mechanical strength for cell attachment and prolong the curcumin release time from liposomes. The *in vitro* drug release profile showed only 17% of curcumin was released from liposome-coated scaffolds after two months compared with 30.9% release of free curcumin, indicating effectively controlled curcumin release. In addition, the MTT assay identified a significant decrease in the number of human osteosarcoma cells (MG-63) resulting in cell viability of just 3.56% after an 11 day incubation, relative to the control. Importantly, whilst the curcumin was able to exert a killing effect on cancer cells the liposome-loaded scaffolds themselves were shown to improve healthy osteoblast cell attachment and promote osteoblast-differentiating abilities, making this a particularly noteworthy study.

5. Conclusions and outlook

The integration of nanomaterials and 3D printing technologies has been rapidly developed and reported in many important biomedical-related fields including regenerative medicine, tissue engineering, cancer research, and medical imaging. This integrated approach is a powerful strategy to potentially overcome the shortcomings of both nanomaterials and 3D printing. The integration of nanomaterials not only promotes the mechanical properties of 3D-printed devices but also provides unique features and additional functions to printed materials. In other words, the introduction of nanomaterials is promoting the biomedical development of 3D printing technology towards the next stage. Overall, 3D-printed materials show great potential for improving compatibility, increasing dispersity, and reducing the toxicity of nanomaterials. In this review, we have highlighted the biomedical properties of nanomaterials, integrated approaches of nanomaterials and 3D printing, and their biomedical applications. Our aim with this review is to inform researchers about the current state of play in regard to nanomaterial use in 3D-printed models and inspire them to develop exciting breakthrough nanotechnological 3D printing devices that can be readily translated for any number of biomedical applications.

However, there are still some limitations to be overcome to meet the requirements for such clinical translation. First, the compatibility between nanomaterials and specific 3D printing technologies is still seen as a challenge. Specifically, the utilization of nanomaterials may be regarded as interference factors that reduce printing efficiency or makes additional unmet demands on the 3D printer. For example, in SLA printing, nanomaterials within an ink reservoir inevitably affect the light penetration and scattering, resulting in a significant decrease in the printing speed. Although nanomaterials often improve the printing speed, resolution, accuracy, and surface finish, the agglomeration of nanomaterials results in uneven spreading of the ink or powder.[147] Also, the toxicity and degradability of nanomaterials inside 3D-printed scaffolds are challenging for certain biomedical applications. Free-floating nanomaterials can easily be transported through the blood circulation and be effectively cleared by the kidney or excreted in feces to reduce the chances of long-term toxicity. However, there is a distinct lack of effective biodegradability in fabricated devices, and this leads to difficulties in releasing nanoparticles from the 3D-printed scaffolds. If the printed implants remain in the body for a long time, nanomaterials will inevitably become a safety hazard. Thus, selecting optimal nanomaterials is an important part of overcoming this limitation. Natural nanomaterials, like liposome nanoparticles and nano-hydroxyapatite, should be more extensively explored in 3D printing instead of nanomaterials with high toxicity and low biocompatibility alongside the use of pH, Thermo, and enzyme responsive scaffolds that allow the stimuli-responsive release of drugs at the targeted lesions.

Despite the current limitations associated with the integration of nanomaterials in 3D printing, it is highly probable that we will soon see nanoparticle-integrated 3D printing scaffolds that stably and robustly produce a superior effect to conventional 3D-printed models. Further to this, it is our hope that these cutting-edge models will be routinely used in an extensive range of applications within a pre-clinical research setting, and more importantly, in the clinic.

Conflicts of interest

There are no conflicts to declare.

Acknowledgements

R. Q. is grateful for the National Health and Medical Research Council (APP1196850), UQ Amplify Women's Academic Research Equity (UQAWARE), UQ Foundation of Excellence Research Award (UQFERA), and Advance Queensland Women's Research Assistance Program (AQWRAP).

References

1 A. A. Giannopoulos, D. Mitsouras, S.-J. Yoo, P. P. Liu, Y. S. Chatzizisis and F. J. Rybicki, *Nat. Rev. Cardiol.*, 2016, **13**, 701–718.

2 A. J. Capel, R. P. Rimington, M. P. Lewis and S. D. Christie, *Nat. Rev. Chem.*, 2018, **2**, 422–436.
3 H.-W. Kang, S. J. Lee, I. K. Ko, C. Kengla, J. J. Yoo and A. Atala, *Nat. Biotechnol.*, 2016, **34**, 312–319.
4 Y. Y. C. Choong, H. W. Tan, D. C. Patel, W. T. N. Choong, C.-H. Chen, H. Y. Low, M. J. Tan, C. D. Patel and C. K. Chua, *Nat. Rev. Mater.*, 2020, **5**, 637–639.
5 N. Shahrubudin, P. Koshy, J. Alipal, M. Kadir and T. Lee, *Heliyon*, 2020, **6**, e03734.
6 N. Doshi and S. Mitragotri, *Adv. Funct. Mater.*, 2009, **19**, 3843–3854.
7 S. Mitragotri and J. Lahann, *Nat. Mater.*, 2009, **8**, 15–23.
8 M. A. Dobrovolskaia and S. E. McNeil, *Nanosci. Technol.*, 2010, 278–287.
9 M. De, P. S. Ghosh and V. M. Rotello, *Adv. Mater.*, 2008, **20**, 4225–4241.
10 L. Deng, Y. Deng and K. Xie, *Colloids Surf., B*, 2017, **160**, 483–492.
11 N. A. Pattanashetti, S. Biscaia, C. Moura, G. R. Mitchell and M. Y. Kariduraganavar, *Mater. Today Commun.*, 2019, **21**, 100651.
12 Y. Zhang, D. Zhai, M. Xu, Q. Yao, H. Zhu, J. Chang and C. Wu, *Biofabrication*, 2017, **9**, 025037.
13 K. C. Hung, C. S. Tseng and S. h Hsu, *Adv. Healthcare Mater.*, 2014, **3**, 1578–1587.
14 J. Zhang, S. Zhao, M. Zhu, Y. Zhu, Y. Zhang, Z. Liu and C. Zhang, *J. Mater. Chem. B*, 2014, **2**, 7583–7595.
15 W. Dang, T. Li, B. Li, H. Ma, D. Zhai, X. Wang, J. Chang, Y. Xiao, J. Wang and C. Wu, *Biomaterials*, 2018, **160**, 92–106.
16 Y. Luo, X. Wei, Y. Wan, X. Lin, Z. Wang and P. Huang, *Acta Biomater.*, 2019, **92**, 37–47.
17 C. Schubert, M. C. Van Langeveld and L. A. Donoso, *Br. J. Ophthalmol.*, 2014, **98**, 159–161.
18 B. C. Gross, J. L. Erkal, S. Y. Lockwood, C. Chen and D. M. Spence, *Anal. Chem.*, 2014, **86**, 3240–3253.
19 M. Hassan, K. Dave, R. Chandrawati, F. Dehghani and V. G. Gomes, *Eur. Polym. J.*, 2019, **121**, 109340.
20 J. dos Santos, R. S. de Oliveira, T. V. de Oliveira, M. C. Velho, M. V. Konrad, G. S. da Silva, M. Deon and R. C. Beck, *Adv. Funct. Mater.*, 2021, **31**, 2009691.
21 S. A. Tofail, E. P. Koumoulos, A. Bandyopadhyay, S. Bose, L. O'Donoghue and C. Charitidis, *Mater. Today*, 2018, **21**, 22–37.
22 N. Shahrubudin, T. C. Lee and R. Ramlan, *Procedia Manuf.*, 2019, **35**, 1286–1296.
23 Ö. Keleş, C. W. Blevins and K. J. Bowman, *Rapid Prototyp. J.*, 2017, **23**, 320–328.
24 E. Mathew, G. Pitzanti, E. Larrañeta and D. A. Lamprou, *Journal*, 2020, **12**, 266.
25 P. Ahangar, M. E. Cooke, M. H. Weber and D. H. Rosenzweig, *Appl. Sci.*, 2019, **9**, 1713.
26 D. K. Tan, M. Maniruzzaman and A. Nokhodchi, *Pharmaceutics*, 2018, **10**, 203.
27 S. Lamichhane, J.-B. Park, D. H. Sohn and S. Lee, *Pharmaceutics*, 2019, **11**, 564.
28 N. Reddy Dumpa, S. Bandari and M. A. Repka, *Pharmaceutics*, 2020, **12**, 52.
29 I. Seoane-Viaño, P. Januskaite, C. Alvarez-Lorenzo, A. W. Basit and A. Goyanes, *J. Controlled Release*, 2021, **332**, 367–389.
30 D. Kokkinis, M. Schaffner and A. R. Studart, *Nat. Commun.*, 2015, **6**, 1–10.
31 P. Robles-Martinez, X. Xu, S. J. Trenfield, A. Awad, A. Goyanes, R. Telford, A. W. Basit and S. Gaisford, *Pharmaceutics*, 2019, **11**, 274.
32 J. Wang, A. Goyanes, S. Gaisford and A. W. Basit, *Int. J. Pharm.*, 2016, **503**, 207–212.
33 M. B. Hoy, *Med. Ref. Serv. Q.*, 2013, **32**, 93–99.
34 J. Zhang, Q. Hu, S. Wang, J. Tao and M. Gou, *Int. J. Bioprint.*, 2020, **6**, 242.
35 A. Diaz Lantada and P. Lafont Morgado, *Annu. Rev. Biomed. Eng.*, 2012, **14**, 73–96.
36 L.-C. Zhang, H. Attar, M. Calin and J. Eckert, *Mater. Technol.*, 2016, **31**, 66–76.
37 S. Hales, E. Tokita, R. Neupane, U. Ghosh, B. Elder, D. Wirthlin and Y. L. Kong, *Nanotechnology*, 2020, **31**, 172001.
38 Y. L. Kong, M. K. Gupta, B. N. Johnson and M. C. McAlpine, *Nano Today*, 2016, **11**, 330–350.
39 P. J. Borm, D. Robbins, S. Haubold, T. Kuhlbusch, H. Fissan, K. Donaldson, R. Schins, V. Stone, W. Kreyling and J. Lademann, *Part. Fibre Toxicol.*, 2006, **3**, 1–35.
40 E. Roduner, *Chem. Soc. Rev.*, 2006, **35**, 583–592.
41 I. Khan, K. Saeed and I. Khan, *Arabian J. Chem.*, 2019, **12**, 908–931.
42 T. A. Campbell and O. S. Ivanova, *Nano Today*, 2013, **8**, 119–120.
43 L. Zhang, G. Ng, N. Kapoor-Kaushik, X. Shi, N. Corrigan, R. Webster, K. Jung and C. Boyer, *Angew. Chem., Int. Ed.*, 2021, **60**, 22664–22671.
44 Y. Xia, B. Gates and Z. Y. Li, *Adv. Mater.*, 2001, **13**, 409–413.
45 Q. Zhang, F. Zhang, S. P. Medarametla, H. Li, C. Zhou and D. Lin, *Small*, 2016, **12**, 1702–1708.
46 Q. Zhang, F. Zhang, X. Xu, C. Zhou and D. Lin, *ACS Nano*, 2018, **12**, 1096–1106.
47 J. H. Kim, W. S. Chang, D. Kim, J. R. Yang, J. T. Han, G. W. Lee, J. T. Kim and S. K. Seol, *Adv. Mater.*, 2015, **27**, 157–161.
48 M. Su, Z. Huang, Y. Li, X. Qian, Z. Li, X. Hu, Q. Pan, F. Li, L. Li and Y. Song, *Adv. Mater.*, 2018, **30**, 1703963.
49 D. Lin, S. Jin, F. Zhang, C. Wang, Y. Wang, C. Zhou and G. J. Cheng, *Nanotechnology*, 2015, **26**, 434003.
50 Q. Mu, L. Wang, C. K. Dunn, X. Kuang, F. Duan, Z. Zhang, H. J. Qi and T. Wang, *Addit. Manuf.*, 2017, **18**, 74–83.
51 L. Zhang, X. Shi, Z. Zhang, R. P. Kuchel, R. Namivandi-Zangeneh, N. Corrigan, K. Jung, K. Liang and C. Boyer, *Angew. Chem., Int. Ed.*, 2021, **60**, 5489–5496.
52 T. D. Ngo, A. Kashani, G. Imbalzano, K. T. Nguyen and D. Hui, *Composites, Part B*, 2018, **143**, 172–196.
53 X. Wang, M. Jiang, Z. Zhou, J. Gou and D. Hui, *Composites, Part B*, 2017, **110**, 442–458.

54 J. Schwartz and A. Boydston, *Nat. Commun.*, 2019, **10**, 1–10.
55 A. K. Miri, D. Nieto, L. Iglesias, H. Goodarzi Hosseinabadi, S. Maharjan, G. U. Ruiz-Esparza, P. Khoshakhlagh, A. Manbachi, M. R. Dokmeci and S. Chen, *Adv. Mater.*, 2018, **30**, 1800242.
56 X. Cui, T. Boland, D. DD'Lima and M. K. Lotz, *Recent Pat. Drug Delivery Formulation*, 2012, **6**, 149–155.
57 C. L. Ventola, *Pharm. Ther.*, 2014, **39**, 704.
58 A. Aimar, A. Palermo and B. Innocenti, *J. Healthc. Eng.*, 2019, **2019**, 5340616.
59 W. Jamróz, J. Szafraniec, M. Kurek and R. Jachowicz, *Pharm. Res.*, 2018, **35**, 1–22.
60 S. Fatima, A. Haleem, S. Bahl, M. Javaid, S. K. Mahla and S. Singh, *Mater. Today: Proc.*, 2021, **45**, 4844–4851.
61 R. Pugh, K. Lloyd, M. Collins and A. Duxbury, *J. Radiother. Pract.*, 2017, **16**, 319–325.
62 J. Banks, *IEEE Pulse*, 2013, **4**, 22–26.
63 L. Mertz, *IEEE Pulse*, 2013, **4**, 12–14.
64 J. Chen, Z. Zhang, X. Chen, C. Zhang, G. Zhang and Z. Xu, *J. Prosthet. Dent.*, 2014, **112**(1088–1095), e1081.
65 L. Mertz, *IEEE pulse*, 2013, **4**, 15–21.
66 S. Bartlett, *Lancet Respir. Med.*, 2013, **1**, 684.
67 I. D. Ursan, L. Chiu and A. Pierce, *J. Am. Pharm. Assoc.*, 2013, **53**, 136–144.
68 A. A. Yaqoob, H. Ahmad, T. Parveen, A. Ahmad, M. Oves, I. M. Ismail, H. A. Qari, K. Umar and M. N. Mohamad Ibrahim, *Front. Chem.*, 2020, **8**, 341.
69 G. Franci, A. Falanga, S. Galdiero, L. Palomba, M. Rai, G. Morelli and M. Galdiero, *Molecules*, 2015, **20**, 8856–8874.
70 T. R. Correia, D. R. Figueira, K. D. de Sá, S. P. Miguel, R. G. Fradique, A. G. Mendonça and I. J. Correia, *Int. J. Biol. Macromol.*, 2016, **93**, 1432–1445.
71 W. Wan, F. Cai, J. Huang, S. Chen and Q. Liao, *J. Mater. Chem. B*, 2019, **7**, 2954–2961.
72 X. Ding, X. He, C. Xue, C. Wu, L. Xie, T. Chen, J. Wei, X. Cheng and X. Wang, *RSC Adv.*, 2016, **6**, 76785–76788.
73 Y. Deng, X. Shi, Y. Chen, W. Yang, Y. Ma, X.-L. Shi, P. Song, M. S. Dargusch and Z.-G. Chen, *Ind. Eng. Chem. Res.*, 2020, **59**, 12123–12135.
74 E. Gutierrez, P. A. Burdiles, F. Quero, P. Palma, F. Olate-Moya and H. Palza, *ACS Biomater. Sci. Eng.*, 2019, **5**, 6290–6299.
75 I. Cockerill, Y. Su, S. Sinha, Y.-X. Qin, Y. Zheng, M. L. Young and D. Zhu, *Mater. Sci. Eng., C*, 2020, **110**, 110738.
76 S. Vial, R. L. Reis and J. M. Oliveira, *Curr. Opin. Solid State Mater. Sci.*, 2017, **21**, 92–112.
77 S. JináLee, J. MináSeok, J. HeeáLee, W. DooáKim, I. KeunáKwon and S. AáPark, *Nanoscale*, 2018, **10**, 15447–15453.
78 J. Hainfeld, D. Slatkin, T. Focella and H. Smilowitz, *Br. J. Radiol.*, 2006, **79**, 248–253.
79 N. Celikkin, S. Mastrogiacomo, X. F. Walboomers and W. Swieszkowski, *Polymers*, 2019, **11**, 367.
80 K. H. Nam, C. B. Jeong, H. Kim, M. Ahn, S. J. Ahn, H. Hur, D. U. Kim, J. Jang, H. J. Gwon and Y. M. Lim, *Adv. Healthcare Mater.*, 2021, **10**, 2100636.
81 S. Laurent and M. Mahmoudi, *Int. J. Mol. Epidemiol. Genet.*, 2011, **2**, 367.
82 Y. Yang, C. Tong, J. Zhong, R. Huang, W. Tan and Z. Tan, *J. Biomed. Mater. Res., Part B*, 2018, **106**, 1827–1841.
83 D.-H. Kim, D. E. Nikles, D. T. Johnson and C. S. Brazel, *J. Magn. Magn. Mater.*, 2008, **320**, 2390–2396.
84 S. Dong, Y. Chen, L. Yu, K. Lin and X. Wang, *Adv. Funct. Mater.*, 2020, **30**, 1907071.
85 H.-Y. Lin, H.-Y. Huang, S.-J. Shiue and J.-K. Cheng, *J. Magn. Magn. Mater.*, 2020, **504**, 166680.
86 H. Ceylan, I. C. Yasa, O. Yasa, A. F. Tabak, J. Giltinan and M. Sitti, *ACS Nano*, 2019, **13**, 3353–3362.
87 U. Bozuyuk, O. Yasa, I. C. Yasa, H. Ceylan, S. Kizilel and M. Sitti, *ACS Nano*, 2018, **12**, 9617–9625.
88 M. Gkagkanasiou, A. Ploussi, M. Gazouli and E. P. Efstathopoulos, *J. Neuroimaging*, 2016, **26**, 161–168.
89 H. Li, Y. Yin, Y. Xiang, H. Liu and R. Guo, *Biomed. Mater.*, 2020, **15**, 045004.
90 S. Wu, Z. Weng, X. Liu, K. Yeung and P. K. Chu, *Adv. Funct. Mater.*, 2014, **24**, 5464–5481.
91 Z. F. Yin, L. Wu, H. G. Yang and Y. H. Su, *Phys. Chem. Chem. Phys.*, 2013, **15**, 4844–4858.
92 A. Nazari, S. Riahi, S. Riahi, S. F. Shamekhi and A. Khademno, *J. Am. Sci.*, 2010, **6**, 98–101.
93 E. E. Totu, A. C. Nechifor, G. Nechifor, H. Y. Aboul-Enein and C. M. Cristache, *J. Dent.*, 2017, **59**, 68–77.
94 S. Chen, J. Yang, K. Li, B. Lu and L. Ren, *Int. J. Food Prop.*, 2018, **21**, 2557–2565.
95 D. Losic and S. Simovic, *Expert Opin. Drug Delivery*, 2009, **6**, 1363–1381.
96 K. Gulati, M. S. Aw, D. Findlay and D. Losic, *Ther. Delivery*, 2012, **3**, 857–873.
97 S. Maher, G. Kaur, L. Lima-Marques, A. Evdokiou and D. Losic, *ACS Appl. Mater. Interfaces*, 2017, **9**, 29562–29570.
98 P. He, H. Zhang, Y. Li, M. Ren, J. Xiang, Z. Zhang, P. Ji and S. Yang, *Mater. Sci. Eng., C*, 2020, **109**, 110551.
99 J. Qin, D. Yang, S. Maher, L. Lima-Marques, Y. Zhou, Y. Chen, G. J. Atkins and D. Losic, *J. Mater. Chem. B*, 2018, **6**, 3136–3144.
100 M. T. Islam, A. Dominguez, B. Alvarado-Tenorio, R. A. Bernal, M. O. Montes and J. C. Noveron, *ACS Omega*, 2019, **4**, 6560–6572.
101 C. M. Cleetus, F. A. Primo, G. Fregoso, N. L. Raveendran, J. C. Noveron, C. T. Spencer, C. V. Ramana and B. Joddar, *Int. J. Nanomed.*, 2020, **15**, 5097.
102 H.-S. Roh, C.-M. Lee, Y.-H. Hwang, M.-S. Kook, S.-W. Yang, D. Lee and B.-H. Kim, *Mater. Sci. Eng., C*, 2017, **74**, 525–535.
103 W. Yang, W. Guo, J. Chang and B. Zhang, *J. Mater. Chem. B*, 2017, **5**, 401–417.
104 L. Zhang, S. Gao, F. Zhang, K. Yang, Q. Ma and L. Zhu, *ACS Nano*, 2014, **8**, 12250–12258.
105 X. Wang, T. Li, H. Ma, D. Zhai, C. Jiang, J. Chang, J. Wang and C. Wu, *NPG Asia Mater.*, 2017, **9**, e376.
106 H. Wang, X. Zeng, L. Pang, H. Wang, B. Lin, Z. Deng, E. L. X. Qi, N. Miao, D. Wang and P. Huang, *Chem. Eng. J.*, 2020, **396**, 125081.

107 T. Daeneke, K. Khoshmanesh, N. Mahmood, I. A. De Castro, D. Esrafilzadeh, S. Barrow, M. Dickey and K. Kalantar-Zadeh, *Chem. Soc. Rev.*, 2018, **47**, 4073–4111.
108 K. Kalantar-Zadeh, J. Tang, T. Daeneke, A. P. O'Mullane, L. A. Stewart, J. Liu, C. Majidi, R. S. Ruoff, P. S. Weiss and M. D. Dickey, *ACS Nano*, 2019, **13**, 7388–7395.
109 S.-Y. Tang, C. Tabor, K. Kalantar-Zadeh and M. D. Dickey, *Annu. Rev. Mater. Res.*, 2021, **51**, 381–408.
110 T. Cole, K. Khoshmanesh and S.-Y. Tang, *Adv. Intell. Syst.*, 2021, **3**, 2000275.
111 H. Li, R. Qiao, T. P. Davis and S.-Y. Tang, *Biosensors*, 2020, **10**, 196.
112 S.-Y. Tang and R. Qiao, *Acc. Mater. Res.*, 2021, **2**, 966–978.
113 W. Xie, F.-M. Allioux, J. Z. Ou, E. Miyako, S.-Y. Tang and K. Kalantar-Zadeh, *Trends Biotechnol.*, 2021, **39**, 624–640.
114 M. D. Dickey, *Adv. Mater.*, 2017, **29**, 1606425.
115 C. Jin, J. Zhang, X. Li, X. Yang, J. Li and J. Liu, *Sci. Rep.*, 2013, **3**, 1–7.
116 Y. Y. Choi, D. H. Ho and J. H. Cho, *ACS Appl. Mater. Interfaces*, 2020, **12**, 9824–9832.
117 S. Veerapandian, W. Jang, J. B. Seol, H. Wang, M. Kong, K. Thiyagarajan, J. Kwak, G. Park, G. Lee and W. Suh, *Nat. Mater.*, 2021, **20**, 533–540.
118 S. Moon, H. Kim, K. Lee, J. Park, Y. Kim and S. Q. Choi, *iScience*, 2021, **24**, 103183.
119 M. Eddaoudi, J. Kim, N. Rosi, D. Vodak, J. Wachter, M. O'Keeffe and O. M. Yaghi, *Science*, 2002, **295**, 469–472.
120 H. Li, M. Eddaoudi, M. O'Keeffe and O. M. Yaghi, *Nature*, 1999, **402**, 276–279.
121 M. Giménez-Marqués, T. Hidalgo, C. Serre and P. Horcajada, *Coord. Chem. Rev.*, 2016, **307**, 342–360.
122 J. Yang and Y. W. Yang, *Small*, 2020, **16**, 1906846.
123 L. Zhong, J. Chen, Z. Ma, H. Feng, S. Chen, H. Cai, Y. Xue, X. Pei, J. Wang and Q. Wan, *Nanoscale*, 2020, **12**, 24437–24449.
124 K. Huo, X. Zhang, H. Wang, L. Zhao, X. Liu and P. K. Chu, *Biomaterials*, 2013, **34**, 3467–3478.
125 X. Shen, Y. Hu, G. Xu, W. Chen, K. Xu, Q. Ran, P. Ma, Y. Zhang, J. Li and K. Cai, *ACS Appl. Mater. Interfaces*, 2014, **6**, 16426–16440.
126 X. Luo, D. Barbieri, N. Davison, Y. Yan, J. D. de Bruijn and H. Yuan, *Acta Biomater.*, 2014, **10**, 477–485.
127 P. Pei, Z. Tian and Y. Zhu, *Microporous Mesoporous Mater.*, 2018, **272**, 24–30.
128 M. Zhao, Y. Wang, Q. Ma, Y. Huang, X. Zhang, J. Ping, Z. Zhang, Q. Lu, Y. Yu and H. Xu, *Adv. Mater.*, 2015, **27**, 7372–7378.
129 S. Zhao, Y. Wang, J. Dong, C.-T. He, H. Yin, P. An, K. Zhao, X. Zhang, C. Gao and L. Zhang, *Nat. Energy*, 2016, **1**, 1–10.
130 W. Dang, B. Ma, B. Li, Z. Huan, N. Ma, H. Zhu, J. Chang, Y. Xiao and C. Wu, *Biofabrication*, 2020, **12**, 025005.
131 S. Shanmugam, J. Xu and C. Boyer, *J. Am. Chem. Soc.*, 2015, **137**, 9174–9185.
132 L. Zhang, C. Wu, K. Jung, Y. H. Ng and C. Boyer, *Angew. Chem.*, 2019, **131**, 16967–16970.
133 Z.-M. Dang, J.-K. Yuan, J.-W. Zha, T. Zhou, S.-T. Li and G.-H. Hu, *Prog. Mater. Sci.*, 2012, **57**, 660–723.
134 S. Pina, J. M. Oliveira and R. L. Reis, *Adv. Mater.*, 2015, **27**, 1143–1169.
135 F. Zou, J. Jiang, F. Lv, X. Xia and X. Ma, *J. Nanobiotechnol.*, 2020, **18**, 1–14.
136 S. Wilks, H. Michels and C. Keevil, *Int. J. Food Microbiol.*, 2005, **105**, 445–454.
137 A. Tripathi, S. Saravanan, S. Pattnaik, A. Moorthi, N. C. Partridge and N. Selvamurugan, *Int. J. Biol. Macromol.*, 2012, **50**, 294–299.
138 F. Auzel, *Chem. Rev.*, 2004, **104**, 139–174.
139 M. Haase and H. Schäfer, *Angew. Chem., Int. Ed.*, 2011, **50**, 5808–5829.
140 K. Nigoghossian, S. Saska, L. M. Christovam, F. Coelho, C. A. G. Beatrice, A. A. Lucas, P. I. Neto, J. V. L. d Silva, A. Tercjak and M. S. Baptista, *J. Braz. Chem. Soc.*, 2020, **31**, 638–652.
141 K. Deng, C. Li, S. Huang, B. Xing, D. Jin, Q. Zeng, Z. Hou and J. Lin, *Small*, 2017, **13**, 1702299.
142 Y. Zhang, L. Zhang, R. Deng, J. Tian, Y. Zong, D. Jin and X. Liu, *J. Am. Chem. Soc.*, 2014, **136**, 4893–4896.
143 Y. Chen, J. Zhang, X. Liu, S. Wang, J. Tao, Y. Huang, W. Wu, Y. Li, K. Zhou and X. Wei, *Sci. Adv.*, 2020, **6**, eaba7406.
144 B. García-Pinel, C. Porras-Alcalá, A. Ortega-Rodríguez, F. Sarabia, J. Prados, C. Melguizo and J. M. López-Romero, *Nanomaterials*, 2019, **9**, 638.
145 J. Liu, T. Tagami and T. Ozeki, *Mar. Drugs*, 2020, **18**, 325.
146 N. Sarkar and S. Bose, *ACS Appl. Mater. Interfaces*, 2019, **11**, 17184–17192.
147 B. Utela, D. Storti, R. Anderson and M. Ganter, *J. Manuf. Process.*, 2008, **10**, 96–104.

